

Ocean Engineering

Optimization of Mooring Line Design Parameters Using Mooring Optimization Tool for FPSO (MooOpT4FPSO) with the Consideration of Integrated Design Methodology --Manuscript Draft--

Manuscript Number:	OE-D-22-01156R2
Article Type:	Full length article
Section/Category:	
Keywords:	Optimization; Mooring line design parameters; FPSO; RegPSO; OrcaFlex; SAFOP
Corresponding Author:	Montasir Osman Universiti Teknologi PETRONAS Bandar Seri Iskandar, MALAYSIA
First Author:	Idris Ahmed Ja'e, PhD in view
Order of Authors:	Idris Ahmed Ja'e, PhD in view Montasir Osman, PhD Anurag Yenduri, Msc Chiemela Victor Amaechi, PhD Zafarullah Nizamani, PhD Akihiko Nakayama, PhD
Abstract:	<p>Optimization of mooring line design parameters of a turret moored FPSO. The Optimization procedure is implemented using a Mooring Optimization Tool for FPSO (MooOpT4FPSO), which is an in-house optimization tool purposely developed for this purpose. The tool is a synchronization of a Regrouping Particle Swarm Optimization (RegPSO) algorithm with commercial software, OrcaFlex. A case study using a validated numerical FPSO model moored with 12 multicomponent mooring lines acted upon by non-collinear wave, wind and current are analyzed using the developed tool. To take into consideration the interaction of the riser system in the optimization procedure, the integrated design methodology was adopted where the riser safe operation (SAFOP) zone diagram combined with the offset diagram is used to visually assess the verification/assessment of the design criteria of both the riser and mooring line. From the optimized results, the application of the tool can help the industry save material (by reduction of line diameter and length) and consequently the overall project cost, in addition to the reduction of payload exerted on the platform. In addition, the tool has an automatic search capability, which is an improvement to the conventional mooring design approach which is based on a trial-and-error approach.</p>
Suggested Reviewers:	<p>John Kurian, PhD Dean of Research & Development at Providence College of Engineering, Providence College john.k@providence.edu.in Because of his knowledge in offshore engineering</p> <p>Do Kyun Kim, PhD Senior Lecturer, Newcastle University do.kim@ncl.ac.uk Because of his knowledge in offshore engineering</p> <p>Idris Ahmed, PhD Senior Lecturer, Bayero University Aidris.civ@buk.edu.ng because of his knowledge in offshore engineering</p>

Civil and Environmental Engineering Department,
Universiti Teknologi PETRONAS,
Bandar Seri Iskandar,
Malaysia.

11th April 2022.

The Editor-in-Chief,
OCEAN Engineering,
Sir,

JOURNAL ARTICLE

I am pleased to submit an original research article entitled “**Optimization of Mooring Line Design Parameters Using Mooring Optimization Tool for FPSO (MooOpT4FPSO) with the Consideration of Integrated Design Methodology**” by Idris Ahmed Ja’e, Montasir Osman Ahmed Ali, Anurag Yenduri, Chiemela Victor Amaechi, Zafarullah Nizamani and Akihiko Nakayama to be considered for publication in Ocean Engineering Journal.

In this manuscript, we optimized the mooring design parameters of a turret moored FPSO. The optimization procedure is implemented using an in-house mooring optimisation tool, named MooOpT4FPSO purposely developed for this purpose. The tool is a synchronisation of a Regrouping Particle Swarm Optimisation (RegPSO) algorithm with commercial software, OrcaFlex. A case study using a validated numerical FPSO model moored with 12 multicomponent mooring lines acted upon by non-collinear wave, wind and current are analysed using the developed tool. To take into consideration the interaction of the riser system in the optimisation procedure, the integrated design methodology was adopted where the riser safe operation (SAFOP) zone diagram combined with the offset diagram is used to visually assess the verification/assessment of the design criteria of both the riser and mooring line. From the optimised results, the application of the tool can help the industry save material (by reduction of line diameter and length) and consequently the overall project cost, in addition to the reduction of payload exerted on the platform.

We believe this manuscript is appropriate for publication by the Journal of Ocean Engineering because the paper has presented a novel optimization tool for turret moored FPSO.

This manuscript has not been published and is not under consideration for publication elsewhere.

Thank you for your consideration!

Sincerely,

Dr Montasir Osman Ahmed Ali

HIGHLIGHTS OF THE ARTICLE

- The Optimization tool (MooOpT4FPSO) has successfully optimized line azimuth angles, line length (for the mid segment), line diameter, and mooring radius of a turret moored FPSO while ensuring platform excursions are maintained within the riser SAFOP, which is very important.
- Application of the tool in mooring design can bring a reduction in line material and consequently the overall project cost, in addition to the reduction of payload exerted on the platform.
- Implementation of the tool will eliminate the traditional trial and error or manual approach in mooring design.
- By utilising the OrcaFlex software, the tool can optimise the mooring design parameter of any turret moored FPSO.

Declaration of interests

The authors declare that they have no known competing financial interests or personal relationships that could have appeared to influence the work reported in this paper.

The authors declare the following financial interests/personal relationships which may be considered as potential competing interests:

Authors Contribution

Idris Ahmed Jae: Conceptualization, Methodology, Software, Validation, Formal Analysis, Writing (original and edit)

Montasir Osman Ahmed Ali: Conceptualization, Methodology, Supervision and project administration

Anurag Yenduri: Methodology, Visualization, and supervision

Chiemela Victor Amaechi: software, Formal Analysis, Data Curation and Visualization

Zafarullah Nizamani: Resources, Visualization and Supervision

Akihiko Nakayama: Resources, Visualization and Akihiko Nakayama

Dear respected Reviewers,

We acknowledged your frank suggestions and comments in trying to make this manuscript fit for publishing in Ocean Engineering Journal.

Thank you

Reviewer #1:

Thank you for the good efforts to the article revision.

1) Please check the title of section 3.2, the authors may forget to delete the number '2.3'.

Authors Response

Thank you for your observations

Numberings, '2.3' and 2.3.1 have been deleted

2) The subtitle of 3.2.1 is no need in section 3.2. Deletion is recommended.

Authors Response

Thank you for your comment

Subtitle of section 3.2.1 has been deleted as recommended.

3) Please check the citation and bibliography can be listed by number, besides alphabetical order.

Authors Response

Thank you for your comment

Citations have been carefully updated. The bibliography is listed corresponding to the citations in the manuscript. We used Endnote for the referencing. Thus, citations and bibliography are automatically updated.

4) Although the authors have clarified the tool is not limited by the type of mooring line system (catenary or taut), it would be better if an optimization case for catenary mooring is added for the integrity and typicality of the mooring system optimization for a turret FPSO.

Authors Response

Thank you for your comment

Cases considering catenary mooring lines have been included in sections 4.3.3,4.3.4, 4.4.3, and 4.4.4.

- Section 4.3.3 present optimization results for 12 catenary lines.
- Section 4.3.4 presents the case of 9 catenary lines
- Sections 4.4.3 presents comparison of the platform offset of the original, optimised (intact and damaged) with SAFOP. This section presents the case of 12 catenary lines
- Section 4.4.4, this section presents the case of 9 catenary lines

Reviewer #2:

Authors reply to reviews are irrelevant.

One of the comments I gave was about the steps of the results to see how they converged. Instead of providing proper reply to the comment, they explained how the method works well on some other problems which we have already know. I wanted to see how it converges by iterating, not the results of some other problems.

Thanks for the comments

Our response in the first revision was based on the

Our response in Revision1, was based on the understanding that the reviewer was referring to the convergence of the tool. Thus, the reason we presented Table 8, which is the validation of the functionality of the RegPSO component of the numerical tool with different iterations across 7 mathematical benchmark models.

On the convergence of the optimization results, we have attached herein a printout of the MATLAB command window showing the iterations and convergence of the optimization results as requested. The results are for the case presented in section 4.3.3

In Section 5, it is written in conclusion #2 that the tool has capability of optimizing of turret FPSO with 9 and 12 mooring lines. In the same section, conclusion #4 repeats same of #2 without expressing number of mooring lines of the system which allows one to understand it as this tool can solve any turret FPSO optimization problem. Is this tool valid for any turret FPSO or only the FPSO which have 9 or 12 mooring lines?

Thank you for the comments

Conclusion have been revised. The tool has the capability of optimising turret FPSO with 12 and 9 mooring lines.

The comment about the overall English writing, design of the Tables and Figures is also not considered. The Tables and Figures are still in different format between each other. Authors added Writing problems remains as same as first draft.

Thank you for the comment

Tables and Figures format as highlighted have been reviewed and updated.

- All figures together with the captions have been centralised.
- All Tables have been centralised and formatted using the same font style, size and spacing.

The manuscript has also been proofread and updated.

Figure 5 has everything what Figure 4 has. What is the purpose of putting additional figure? Figures 9 and 10 has same problem.

Thank you for the comment

Figures 4 and 9 have been removed.

Table 1, 2 and 3 has different formats. It would be best to use same format for all instead of using 3 different formats.

Thank you for the comment

Table format have been unified as recommended.

```
AUTOMATIC INPUT VALIDATION
PSO settings:
Utilizing RegPSO:
Global Best (Gbest) PSO
8 iterations maximum (per grouping)
8 iterations maximum (total over all groupings)
Regrouping triggered when normalized swarm radius, "stag_thresh," = ✓
0.00011
Regrouping factor: 1.2/stag_thresh = 10909.0909
Position clamping inactive.
Velocity reset inactive.
Velocities clamped to 50% of the range on each dimension.
History, "ghist," of global bests active.
History, "phist," of personal bests active.
History, "fhist," of all function values active.
History, "vhist," of all velocities active.
1 trial(s)
9 particles
Inertia weight linearly varied from 0.9 to 0.4 per grouping.
Cognitive acceleration coefficient, c1: 1.49618
Social acceleration coefficient, c2: 1.49618
OrcMATItrial_12: 7 dimensions
Range on Dimension 1: [40.000000, 50.000000]
Range on Dimension 2: [130.000000, 140.000000]
Range on Dimension 3: [220.000000, 230.000000]
Range on Dimension 4: [310.000000, 320.000000]
Range on Dimension 5: [2738.000000, 2788.000000]
Range on Dimension 6: [0.150000, 0.170000]
Range on Dimension 7: [2148.000000, 2198.000000]
Threshold required for success: 30
"OnOff_Terminate_Upon_Success" active.

fg = 83.6877
reg_fact = 10909.0909
stag_thresh = 0.00011
g = 45 138 223 316 2732 0.153 2179
range_IS = 10 10 10 10 50 0 50
range_IS_check: 0 0 0 0 0 0 0
RegPSO_grouping_counter = 1

fg = 71.7746
reg_fact = 10909.0909
stag_thresh = 0.00011
g = 51 137 218 321 2712 0.158 2156
range_IS = 10 10 10 10 50 0 50
range_IS_check: 0 0 0 0 0 0 0
```



```
range_IS % of prev: 100 100 100 100 100 100 100
RegPSO_grouping_counter = 2
```

```
fg = 52.7746
reg_fact = 10909.0909
stag_thresh = 0.00011
g = 51 138 224 317 2709 0.161 2141
range_IS = 10 10 10 10 50 0 50
range_IS_check: 0 0 0 0 0 0 0
range_IS % of prev: 100 100 100 100 100 100 100
RegPSO_grouping_counter = 3
```

```
fg = 47.3911
reg_fact = 10909.0909
stag_thresh = 0.00011
g = 55 133 228 313 2701 0.167 2109
range_IS = 10 10 10 10 50 0 50
range_IS_check: 0 0 0 0 0 0 0
range_IS % of prev: 100 100 100 100 100 100 100
RegPSO_grouping_counter = 4
```

```
fg = 41.2945
reg_fact = 10909.0909
stag_thresh = 0.00011
g = 57 134 230 314 2677 0.161 2109
range_IS = 10 10 10 10 50 0 50
range_IS_check: 0 0 0 0 0 0 0
range_IS % of prev: 100 100 100 100 100 100 100
RegPSO_grouping_counter = 5
```

```
fg = 33.2945
reg_fact = 10909.0909
stag_thresh = 0.00011
g = 60 134 231 314 2654 0.158 2098
range_IS = 10 10 10 10 50 0 50
range_IS_check: 0 0 0 0 0 0 0
range_IS % of prev: 100 100 100 100 100 100 100
RegPSO_grouping_counter = 6
```

```
fg = 30.2356
reg_fact = 10909.0909
stag_thresh = 0.00011
g = 61 135 232 317 2646 0.152 2088
range_IS = 10 10 10 10 50 0 50
range_IS_check: 0 0 0 0 0 0 0
```

```
range_IS % of prev: 100 100 100 100 100 100 100  
RegPSO_grouping_counter = 7
```

```
objective=OrcMAT1trial_12, dim=7, np=9, c1=1.4962, c2=1.4962, w_i=0.9, ✓  
w_f=0.4, vmax=50% of the range of the search space per dimension  
Number of Successful Trials: 0  
Number of Unsuccessful Trials: 1  
# of iterations = 8  
fg = 30.2356  
time_elapsed = 18060.9478  
>>
```

Optimization of Mooring Line Design Parameters Using Mooring Optimization Tool for FPSO (MooOpT4FPSO) with the Consideration of Integrated Design Methodology

Idris Ahmed Ja'e^{1,2}, Montasir Osman Ahmed Ali^{1,*}, Anurag Yenduri³, Chiemela Victor Amaechi^{4,5}, Zafarullah Nizamani⁶ and Akihiko Nakayama⁶

¹ Civil and Environmental Engineering Department, Universiti Teknologi PETRONAS, Bandar Seri Iskandar, Perak 32610, Malaysia. idris_18001528@utp.edu.my

² Department of Civil Engineering, Ahmadu Bello University, Zaria, Kaduna State, 810107, Nigeria

³ Global Engineering Centre, Subsea Engineering, TechnipFMC, India, 600032, Chennai, yendurianurag@gmail.com

⁴ Department of Engineering, Lancaster University, Lancaster, LA1 4YR, UK. c.amaechi@lancaster.ac.uk

⁵ Standards Organisation of Nigeria (SON), 52 Lome Crescent, Wuse Zone 7, Abuja, 900287, Nigeria

⁶ Department of Environmental Engineering, Universiti Tunku Abdul Rahman (UTAR), 31900, Kampar, Perak, Malaysia; zafarullah@utar.edu.my, akihiko@utar.edu.my

*Correspondence: montasir.ahmedali@utp.edu.my.

Abstract

Optimisation of mooring line design parameters including line azimuth angles, line diameter, line length and mooring radius is presented for a turret-moored FPSO. The optimisation procedure is implemented using a Mooring Optimisation Tool for FPSO (MooOpT4FPSO), which is an in-house optimisation tool purposely developed for this purpose. The tool is a synchronisation of the Regrouping Particle Swarm Optimisation (RegPSO) algorithm with commercial software, OrcaFlex. Case studies using a validated numerical FPSO model moored with multicomponent mooring lines acted upon by non-collinear wave, wind and current were analysed using the developed tool. To take into consideration the interaction of the riser system in the optimisation procedure, the integrated design methodology was adopted where the riser safe operation (SAFOP) zone diagram combined with the offset diagram is used for the verification/assessment of the design criteria of the risers and mooring lines. The optimized FPSO model offsets in eight directions are found to be within the riser safe operation zone. Based on the results, the tool was able to simultaneously optimise the mooring line diameter, line length, mooring radius, and azimuth angles of the turret FPSO to achieve a specific offset. Application of the tool can help the industry save material (by reduction of line diameter and length) and consequently the overall project cost, in addition to the reduction of structural payload exerted on the platform. Furthermore, the tool has an automatic search capability, which is an improvement to the conventional mooring design approach that is based on a trial-and-error approach.

1
2
3
4 34 **Keywords:** Optimization, Mooring line design parameters, FPSO, RegPSO, OrcaFlex, SAFOP
5

6
7 35 **1 Introduction**

8 36 Mooring system design entails consideration of several factors including the composition of the
9 37 mooring lines, type of platform to be moored, environmental conditions and the time the platform
10 38 will remain anchored in position. Dynamic positioning systems, tethers, mooring lines, or a
11 39 combination of both are used to maintain floating platforms in position. As a result, the mooring
12 40 system's ability to maintain the platform in place has a significant influence on the integrity of the
13 41 risers and the floating platform in general. Hence, the efficiency of the mooring system is largely
14 42 dictated by the mooring line design parameters, including mooring line material, line length,
15 43 azimuth angles, diameter, line pretension, mooring radius etc. However, the selection of these
16 44 design parameters in the currently available procedure is based on a trial-and-error/manual
17 45 approach which depends mainly on the experience of the engineer, thereby making it extremely
18 46 time-consuming[1-3]. In addition, the moorings and risers are designed separately with little
19 47 interaction between the two design teams and mostly using uncoupled analysis[2, 4]. The selection
20 48 of maximum platform offset in both intact and damaged conditions is also done arbitrarily
21 49 irrespective of the direction. The risers are subsequently designed to satisfy their functional
22 50 requirement by considering the same offset. This indicates the target offset values as the only
23 51 connection that links the mooring and riser designs[1].
24
25
26
27
28

29
30 52 Hence, the increased application of FPSOs in deeper waters necessitates the need for an optimum
31 53 mooring design that ensures minimum platform horizontal excursion during operation[5]. This is
32 54 important because substantial platform excursions place an enormous constraint on the workability
33 55 of offshore floating structures. Thus, an optimum mooring system can be achieved by automating
34 56 the search component of the mooring design variable in the design procedure to minimise time and
35 57 effort by eliminating the rigorous trial and error approach, and by considering the mooring design
36 58 variables as optimisation variables.
37
38

39
40 59 To actualise this, several studies on the optimization of mooring line design parameters utilising
41 60 different optimization techniques have been conducted to address the optimization of the mooring
42 61 system. Maffra et al., [6] were the first to apply the Genetic Algorithm (GA) in mooring system
43 62 optimization, with the primary objective of minimising offset of a spread moored vessel through
44 63 the optimisation of the mooring line radius. A mooring pattern optimization of a vessel with a
45 64 multi-point mooring system was presented in [7] using the Steady-State Genetic Algorithm
46 65 (SSGA). Also, Mehdi and Rezvani [5] proposed another mooring optimisation procedure using a
47 66 different variant of GA called Constrained Genetic Algorithm (CGA), the primary objective was
48 67 to minimise platform offset in surge and sway directions by optimizing azimuth angle, mooring
49 68 radius and the line length. Unlike the preceding procedure, Liang et al [8] proposed a multi-
50 69 objective procedure utilising the Non-dominated Sorting Genetic Algorithm II (NSGA-II) to
51 70 optimise several mooring design variables in addition to the platform offset and having the
52 71 capability of providing multiple optimal mooring design.
53
54
55
56

57 72 The application of the Particle Swarm Optimization (PSO) technique was first used for mooring
58 73 line optimization by [9] with the objective function of minimising platform offset by considering
59 74 mooring radius and line azimuth angles as the optimisation parameters. An appreciable reduction
60
61

1
2
3
4 75 in platform offset was recorded in the range of 30% and 60% for the two models considered in the
5 76 work. Furthermore, Monteiro et al [10] assess the implementation of an improved PSO (POSI)
6 77 technique using line mooring radius, azimuth angle, pretension and line material as optimisation
7 78 variables. The PSOI, when compared with the standard PSO is reported to have an improved
8 79 convergence rate which is achieved by the application of a velocity update component. The
9 80 integrated mooring-riser design methodology was also adopted where the riser safe operation
10 81 (SAFOP) zone diagrams in combination with the mooring line offset diagrams were used to
11 82 account for the integrity of the risers. The application of a variant of the PSO algorithm associated
12 83 with an ϵ -constrained was also applied [11] for the optimisation of deep-water semisubmersible
13 84 platform using mooring radius, line length and pretension as optimisation variables. However, this
14 85 procedure is an improvement of the one presented in [10] with the introduction of a constrained
15 86 function to efficiently handle constraints and enhance the evaluation of candidate solutions by
16 87 adopting full non-linear time-domain FE simulations with a coupled model. A more complex
17 88 approach considering asymmetric mooring configurations was considered in [12] taking each of
18 89 the line azimuth angles and mooring radius as optimization variables. The study compares the
19 90 performance of differential evolution and PSO based on their convergence capability. This was
20 91 implemented as a spread mooring system of a deep-water semi-submersible platform. In recent
21 92 times, Montasir *et al.*, [3] proposed a standalone mooring optimisation tool based on quasi-static
22 93 analysis. The line azimuth angle was used as an optimization variable and successfully
23 94 implemented using PSO. The proposed tool has optimised offset of a truss spar offset by up to
24 95 72% when compared with the original model. However, most of the procedures presented utilised
25 96 either static or dynamic in the analysis of mooring lines.

26
27
28
29
30
31
32
33
34 97 Over the years, the interaction between mooring lines and risers has been recognised as an
35 98 important design consideration, particularly in deep-water operations [11, 13-16]. As a result, an
36 99 integrated design methodology has been demonstrated as a better alternative, where the risers,
37 100 moorings, and floaters are all analysed simultaneously to create a SAFOP and offset diagrams for
38 101 the riser and moorings respectively. The inclusion of risers in the analysis of floating platforms
39 102 has been reported as having a significant influence on their natural periods, damping, as well as
40 103 slow drift responses [17]. In another study [18], the inclusion of risers in the analysis was found to
41 104 have considerable contributions to surge/sway coupling, and as a result the low-frequency motion
42 105 response. For this reason, the integrated riser-mooring design methodology was regarded as
43 106 potentially beneficial in deep water platform operations, particularly in terms of the overall system
44 107 safety, response, and cost[14].
45 108 By incorporating all the components in a single model throughout the study, the technique enable
46 109 s for efficient incorporation of the interaction between the riser, mooring, and platform [12, 18].
47 110 Furthermore, previous studies have demonstrated the inclination of the oil and gas industries
48 111 toward full integration of the mooring and riser design procedure[4, 19].

49
50
51
52
53
54 112 Thus, this paper presents an optimisation procedure of mooring line design parameters using the
55 113 Mooring Optimisation Tool for FPSO (MooOpT4FPSO). The tool is an in-house optimization tool,
56 114 which is an integration of the Regrouping Particle Swarm Optimization (RegPSO) algorithm and
57 115 OrcaFlex. The tool has the capability of optimising mooring line parameters of turret FPSO
58 116 supported with 12 or 9 mooring lines. In addition, the tool is configured to take into consideration

of the mooring line parameters, it is not limited by the position of the turret or the type of mooring line system (catenary or taut), thus can be utilised for both internal and external turret. Utilizing the tool, mooring line design parameters; mooring line diameter, line length (middle segment), mooring radius, and azimuth angles of a turret FPSO were simultaneously optimised. The integrated mooring-riser methodology was incorporated to consider the interaction of the riser in the procedure. The paper considered twelve mooring lines azimuth angles, line diameter, mooring radius, and line length as optimization variables. The superimposition of the riser safe operation (SAFOP) zone and the offset diagram reveals the optimised mooring parameters as sufficient in maintaining platform offset within the SAFOP Apart from successfully having the capability of optimising the platform offset, the tool has the flexibility of utilising the robust capability of the OrcaFlex software utilising both static and dynamic analysis.

1.1 Selection of Optimization variables

The mooring system considered in this study is an internal turret consisting of taut and catenary mooring lines. This version of MooOpT4FPSO has the capability of optimising mooring line parameters of turret FPSO with 12 and 9 lines, i.e., 4x3 and 3x3 mooring configuration respectively as illustrated in Figures 1(a, b). Each of the lines comprises a chain-polyester -chain segment distributed equally and at the same pretension characteristic value of 1420kN. The mid-section of each of the mooring lines is of the same length and diameter. Thus, the mooring line design variable of each line identified to influence the performance of the mooring system was adopted as the optimization variable. For each of the mooring configurations, the azimuth angles of the central lines of each group, i.e., lines #1,2,3,4 for 4x3 or lines #1,2,3 for 3x3, are considered optimization parameters. Thus, MooOpT4FPSO considers a total of 7 or 6 mooring line parameters as optimisation parameters, i.e., 4 or 3 azimuth angles, in addition to mooring radius, mooring line length (of mid-segment) and line diameter. The case is automatically selected depending on the number of mooring lines defined by the user.

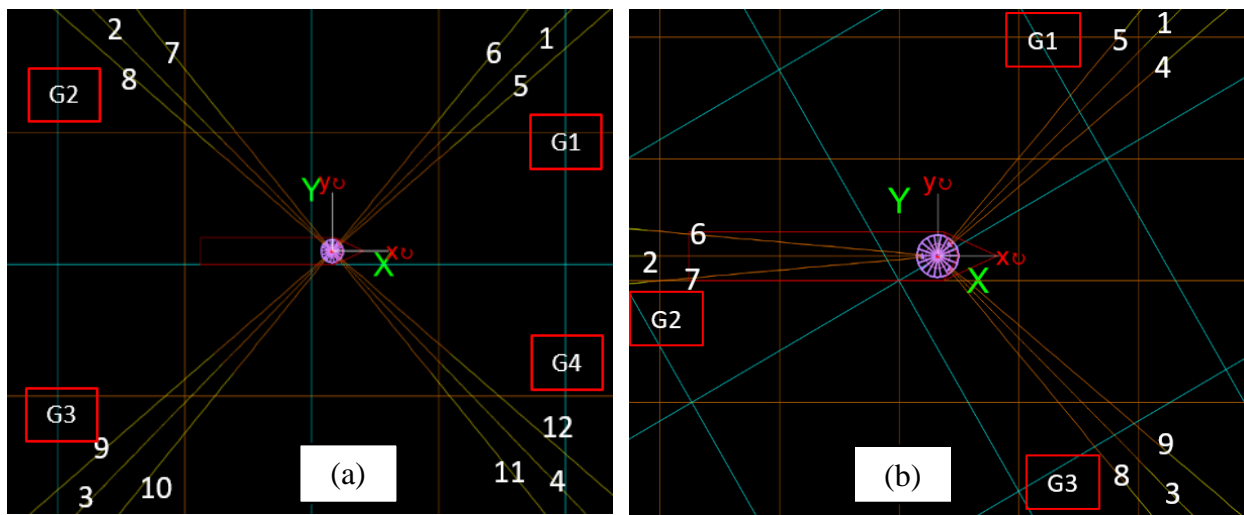


Figure 1: Layout of turret mooring configuration: (a) 4 x 3 configuration (b) 3 x 3 configuration

1.2 Objective function

The problem presented here is a typical constrained optimisation problem, expressed mathematically in Equation 1. The aim is to minimize the objective function $f(x)$ which in this case is the FPSO surge offset. Thus, the primary objective of the optimization procedure is to optimise line parameters that will minimise surge offset of turret FPSO, which has been identified as the most sensitive response.

$$\text{minimize } f(\text{offset}) \quad (1)$$

$$\text{subject to } g_i(\text{offset}) \leq \text{threshold of success}, \quad i, \dots, m$$

Where the *threshold of success* is the maximum allowable platform offset defined for the problem, while $g_i(\text{offset})$, is the global best platform offset for each iteration.

The integrated riser-mooring design methodology elaborated in [1, 14] and adopted in [2] has been incorporated herein. Adopting this approach as a component of the optimization procedure is considered more realistic in terms of ensuring the interaction of risers is taken into consideration. This methodology ensures the platform excursion/offset is maintained within the riser safe operation zone (SAFOP).

Thus, the objective of the integrated riser-mooring design methodology is expressed in Equation (2)

$$f = \frac{\sum_{i=1}^{ndir} SAFOP(i) - \text{platform offset}(i)}{ndir} \quad (2)$$

where, i is the number of directions considered ($i = 1, ndir$), which should be at least 8, $SAFOP(i)$ is the riser safe operation zone in each direction, i recorded in meters, while $\text{platform offset}(i)$ is the platform excursion obtained using the mooring system, and in the same directions.

1.3 Constraints

The maximum allowable mooring tensions are based on the guidance provided in section 7.2 of the API-RP-2SK[20] specifying 60% and 80% of the minimum breaking load (MBL) when considering dynamic analysis in intact and damage conditions respectively. Thus, the tension constraints are expressed in Equations (3).

$$CTsn_{max} = \begin{cases} \frac{Tsn_{max}}{MBL} - 0.6, & \text{if } \frac{Tsn_{max}}{MBL} \geq 0.6 \\ 0, & \text{Otherwise} \end{cases} \quad (3)$$

Where, Tsn_{max} is the maximum mooring tension in all lines of a given candidate solution.

2 The Optimisation Tool

2.1 Mooring Optimization Tool for FPSO

The in-house optimization tool named Mooring Optimization Tool for FPSO (MooOpT4FPSO) is a numerical optimization tool developed to optimize mooring line design parameters of turret moored FPSO. The tool is an integration of a Regrouping Particle Swarm Optimisation (RegPSO)

1
2
3
4
5
6
7
8
9
10
11
12
13
14
15
16
17
18
19
20
21
22
23
24
25
26
27
28
29
30
31
32
33
34
35
36
37
38
39
40
41
42
43
44
45
46
47
48
49
50
51
52
53
54
55
56
57
58
59
60
61
62
63
64
65

187 algorithm with OrcaFlex. This version of MooOpT4FPSO has the capability of simultaneously
188 optimizing azimuth angles, mooring line lengths, line diameter and mooring radius of an FPSO
189 turret mooring system consisting of 9 and 12 mooring lines.

190 MooOpT4FPSO communicate with OrcaFlex in the MATLAB environment through the dynamic
191 link library. Implementation of the optimization procedure includes a complete definition of the
192 FPSO model including the mooring system and environmental loading in OrcaFlex. The OrcaFlex
193 data file is then utilised by the RegPSO algorithm in the MATLAB environment to initialise and
194 assign the mooring line parameters to each line in the OrcaFlex model from a user-defined range.
195 The initialisation of the population of candidate solutions is randomly generated and iteratively
196 updated in the process. For each iteration, dynamic analysis is performed, and a set of mooring
197 line parameters is saved. In each case, individual candidate solutions are evaluated to assess their
198 fitness by the objective function which in turn guides the search process to an optimum solution[1].
199 This procedure is repeated based on the defined number of particles and iterations until an
200 optimised solution is obtained. An optimised solution here refers to mooring line parameters that
201 yield the minimum platform offset. Figure 2 illustrates the data flow diagram of the optimization
202 tool.

203 The developed optimisation tool has an interactive Graphical User Interphase which as illustrated
204 in Figure 3 has 5 major components, namely: (1) the OrcaFlex Path; where the user specifies the
205 path of OrcaFlex on the computer (2) User-defined input; this is where the user defines the
206 optimization and line parameters. (3) The Run, Plot, and Log tabs. (4) Outcomes of optimization;
207 here the optimized mooring line parameters are displayed, and (5) the plot area; the plan of
208 optimized lines with their azimuth angles are displayed.

209 Firstly, implementation of the optimization procedure requires the user to define the OrcaFlex path
210 on the computer. Secondly, the mooring design parameters and optimization settings are defined.
211 Using the run tab, the optimization process is started. Upon completion of the optimization process,
212 the plot is generated using the plot tab. To view the detail of optimization settings or error reports
213 the Log tab is used.

1
2
3
4
5
6
7
8
9
10
11
12
13
14
15
16
17
18
19
20
21
22
23
24
25
26
27
28
29
30
31
32
33
34
35
36
37
38
39
40
41
42
43
44
45
46
47
48
49
50
51
52
53
54
55
56
57
58
59
60
61
62
63
64
65

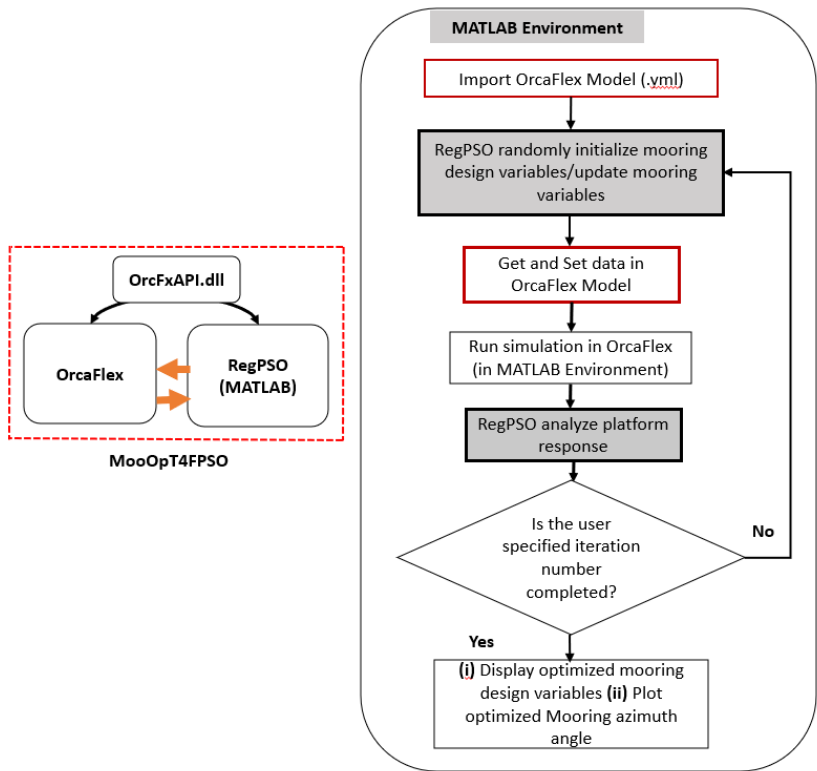


Figure 2: Data flow working diagram of the optimisation tool (MooOpt4FPSO)

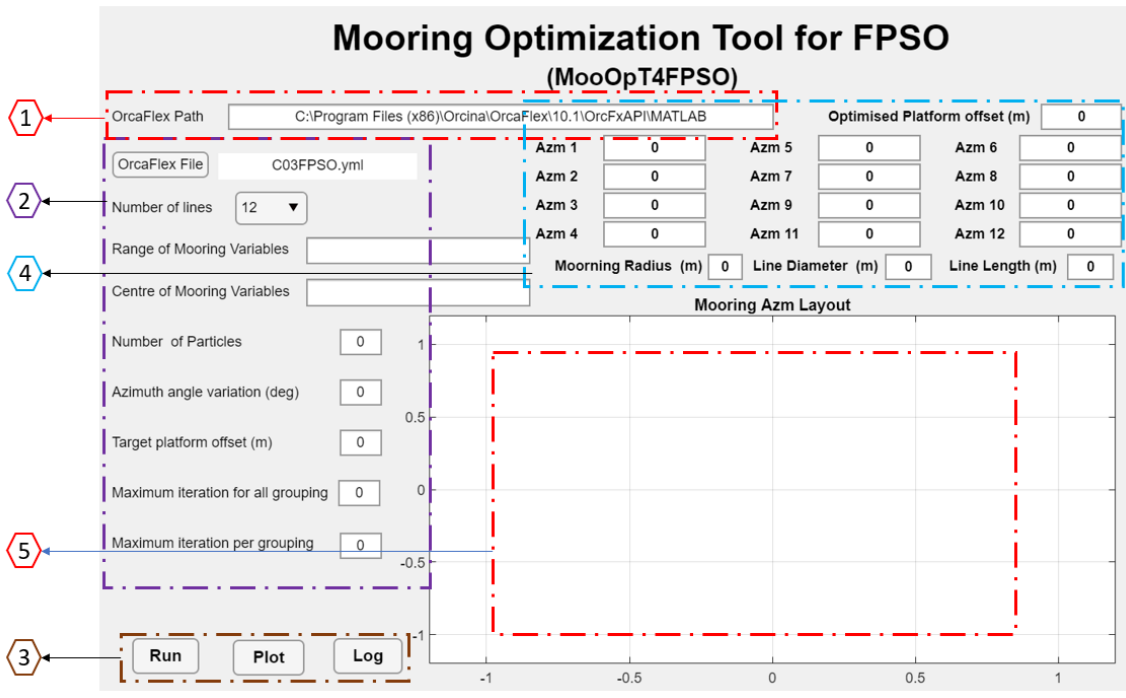


Figure 3: Graphical User Interface of MooOpt4FPSO illustrating the major component

1
2
3
4 218
5
6 219
7
8 220
9 221
10 222
11 223
12 224
13
14 225
15 226
16 227
17 228
18 229
19 229
20 230
21 231
22 232
23 233
24 233
25 234
26 235
27 236
28 237
29 238
30 238
31 239
32 240
33 241
34 241
35 242
36 243
37 244
38 245
39 246
40 246
41 247
42 248
43
44
45
46
47
48
49
50
51
52
53
54
55
56
57
58
59
60
61
62
63
64
65

2.2 Regrouping Particle Swarm Optimisation

The Regrouping Particle Swarm Optimization (RegPSO) technique is a variant of the PSO developed to address the problem of premature convergence identified as a shortcoming of the standard PSO algorithm [21]. The algorithm has the computational capability to identify when premature convergence (viz, stagnation) occurs and regroup the particle into a new search space large enough to allow for an efficient search to enable them to escape stagnation and allow the entire swarm to continue making progress rather than restarting as proposed in other studies [22]. It is important to note that the standard PSO is effective before being prematurely converged. Thus, the RegPSO algorithm still utilizes the original position and velocity update equations. Hence the main improvement is to liberate the swarm from premature convergence via an automatic regrouping mechanism. Figure 4 illustrates the flow chart of the RegPSO algorithm.

All particles are randomly picked from all the problem dimensions toward the global best by using the update Equations in 4 and 5.

$$\vec{x}_i(k + 1) = \vec{x}_i(k) + \vec{v}_i(k + 1) \tag{4}$$

$$\begin{aligned} \vec{v}_i(k + 1) = w\vec{x}_i(k) + c_1\vec{r}_1(k) \circ (\vec{p}_i(k) - \vec{x}_i(k)) + c_2\vec{r}_2(k) \\ \circ (\vec{g}_i(k) - \vec{x}_i(k)) \end{aligned} \tag{5}$$

Where k is the current iteration, \vec{v}_i is the velocity vector, \vec{x}_i is the position vector of particle i while w is the static inertia weight. c_1 and c_2 stand for cognitive and social acceleration coefficients respectively, \vec{p}_i is the personal best of particle i and \vec{g}_i the global best of the swarm. The \vec{r}_1 and \vec{r}_2 are n -dimensional column vectors consisting of pseudo-random numbers selected from a uniform distribution.

1
2
3
4
5
6
7
8
9
10
11
12
13
14
15
16
17
18
19
20
21
22
23
24
25
26
27
28
29
30
31
32
33
34
35
36
37
38
39
40
41
42
43
44
45
46
47
48
49
50
51
52
53
54
55
56
57
58
59
60
61
62
63
64
65

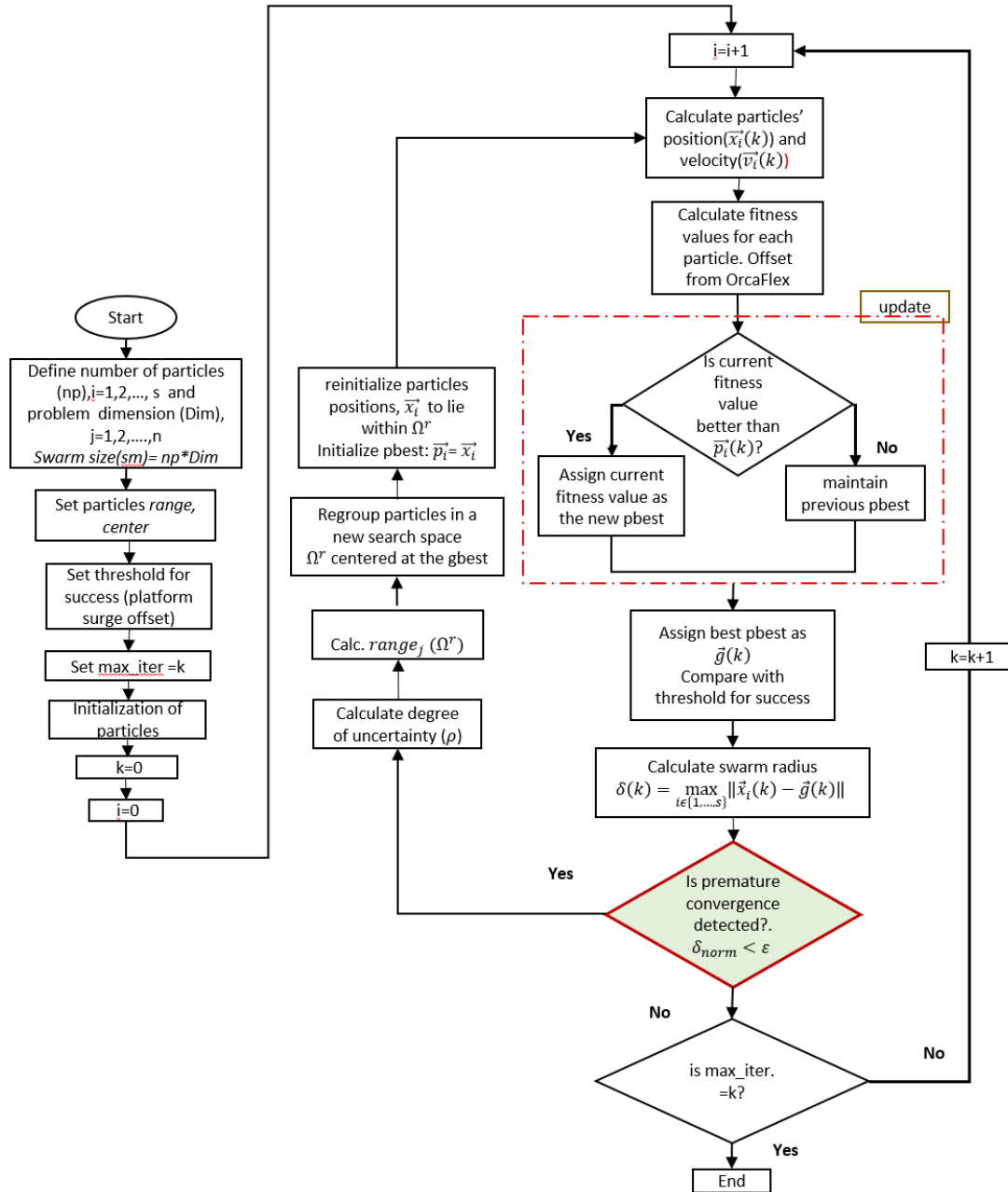


Figure 4: Flow chart of RegPSO algorithm

2.2.1 Detection of Premature Convergence

Depending on the number of particles defined in the process, some particles may fail to find a better solution (i.e., a new global best) over a long simulation time, in which case, the particle will tend to continue to move closer to the unchanged global best until all other particles eventually prematurely converged (occupy the same location in space), thereby approximating a local solution rather than a global one. Consequently, progress toward the global best will cease and the process will instead continue to refine the local minimizer with no room for further improvement.

For this reason, the RegPSO determine the distance between the particles as a measure of how close they are to each other to monitor when they eventually converged to the same region or stagnate. This occurrence (premature convergence) is detected from the measurement of maximum swarm radius between particles using Equation 6, initially introduced by Van den Bargh [23]. For each iteration, the swarm radius $\delta(k)$ is calculated in the n- dimensional space of any particle from the global best.

$$\delta(k) = \max_{i \in \{1, \dots, s\}} \|\vec{x}_i(k) - \vec{g}(k)\| \quad (6)$$

If Ω is considered as the search space and the range of particle dimensions represented by the vector, $\overline{range}(\Omega)$. Then, the diameter of the search space is taken as $dia(\Omega) = \|\overline{range} \Omega\|$. The particles are considered too close to each other when the normalized swarm radius (δ_{norm}) is less than the stagnation threshold (ε) as depicted in Equation (7).

$$\delta_{norm} = \frac{\delta(k)}{dia(\Omega)} < \varepsilon, \text{ where } \varepsilon = 1.1 \times 10^{-4} \quad (7)$$

2.2.2 Regrouping of Swarm

Once the condition in Equation (7) is met (i.e., premature convergence detected), the swarm is automatically regrouped into a new search space centred on the global best, using the regrouping factor shown in Equation (8).

$$\rho = \frac{6}{5\varepsilon} \quad (8)$$

The range of each problem dimension defining the new search space, Ω^r are determined by either the magnitude of the regrouping factor, ρ , or the degree of uncertainty inferred on each dimension from the maximum deviation from the global best.

It is important to state here that the degree of uncertainty on each of the dimensions overall particles is computed using Equation (6) while Equation (9) is used to compute the maximum deviation of any one particle.

$$range_j(\Omega^r) = \min \left(range_j(\Omega^r), \rho \max_{i \in \{1, \dots, s\}} |x_{i,j}(k) - g_j(k)| \right) \quad (9)$$

In each case, each particle is randomly regrouped about the global best within the new search space (Ω^r) according to equation (7), this process makes the randomized particle remain within the Ω^r with respect to the defined lower and upper bounds defined in Equations (12) and (13).

$$\vec{x}_i(k+1) = \vec{g}_i(k) + \vec{r}_i \cdot \overline{range}(\Omega^r) - \frac{1}{2} \cdot \overline{range}(\Omega^r) \quad (10)$$

Where, \vec{r}_i is a vector of the problem dimension

$$[r_1, r_2, \dots, r_n] \quad (11)$$

1
2
3
4
5
6
7
8
9
10
11
12
13
14
15
16
17
18
19
20
21
22
23
24
25
26
27
28
29
30
31
32
33
34
35
36
37
38
39
40
41
42
43
44
45
46
47
48
49
50
51
52
53
54
55
56
57
58
59
60
61
62
63
64
65

$$297 \quad x_j^{L,r} = g_j - \frac{1}{2} range_j(\Omega^r) \quad (12)$$

$$298 \quad x_j^{U,r} = g_j + \frac{1}{2} range_j(\Omega^r) \quad (13)$$

300 L and U in Equations 9 and 10 represent lower and upper limits respectively.

301 Once the regrouping of the particle is implemented as highlighted in the preceding section, the
302 standard PSO continues as usual. This procedure is repeated iteratively.

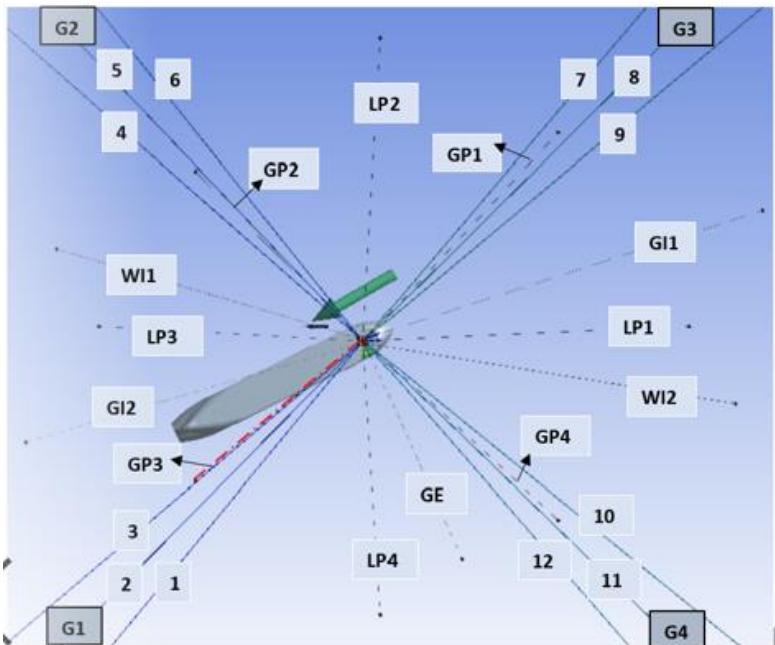
303 2.3 OrcaFlex

304 OrcaFlex is a 3D non-linear finite element software used for the design and analysis of offshore
305 oil and gas structures and Marine systems such as mooring systems, risers, and marine renewables.
306 It has the capabilities of performing Static and dynamic analysis, fatigue analysis and modal
307 analysis, etc. It also has the capability of implementing both quasi-dynamic and fully coupled
308 analysis.

309 3 Description of Model

310 3.1 The FPSO Model

311 In implementing the optimisation procedure, a validated turret moored FPSO model was used as
312 in[24]. The model consists of 12 multi-component mooring lines configured into 4 groups, each
313 group consisting of 3 lines, in addition to 13 steel catenary risers as shown in Figure 5. The FPSO,
314 mooring line and riser system design parameters are depicted in Tables 1, 2 and 3.



316
317 Figure 5: Layout of Mooring-riser systems of turret FPSO

Table 1: FPSO main design parameter [24]

Parameter	Symbol	Unit	Quantities
Vessel size		kDWT	200
Length between perpendicular	L_{pp}	m	310
Breadth	B	m	47.17
Height	H	m	28.04
Draft (80% loaded)	T	M	15.121
Displacement	V	MT	186051
Block coefficient	C_b		0.85
Surge centre of gravity from turret	CGx	m	-109.67
Heave centre of gravity from mwl	CGy	m	-1.8
Frontal wind area	A_F	m ²	4209.6
Transverse wind area	A_T	m ²	16018.6
Roll radius of gyration at CG of turret	R_{xx}	m	14.036
Pitch radius of gyration at CG of turret	R_{yy}	m	77.47
Yaw radius of gyration at CG of turret	R_{zz}	m	79.3
Turret in center line behind F_{pp}	Xtur	m	38.75
Turret diameter	Dtur	m	15.85
Turret elevation below tanker base		m	1.52

Table 2: Mooring line Details [24]

Legend	Top Segment	Middle Segment	Lower Segment
Type	Chain	Polyester	Chain
Diameter(mm)	95.3	160	95.3
Length (m)	91.4	2438	91.4
Wet weight (kg/m)	164.63	4.5	164.63
Effective Modulus (kN)	820900	168120	820900
Breaking Load (kN)	7553	7429	7553
Normal drag coefficient, C_{DN}	2.45	1.2	2.45
Normal added inertia coefficient, C_{IN}	2.0	1.15	2.0

Table 3:Particulars of Steel Catenary Risers

	LP	GP	WI	GI	GE
Top tension (kN)	1112.5	609.7	2020.0	1352.8	453.9
Outer diameter(mm)	444.5	386.1	530.9	287.0	342.9
EA (kN)	18.3 x10 ⁶	10.3 x10 ⁶	18.6 x10 ⁶	31.4 x10 ⁶	8.6 x10 ⁶
Wet Weight (N/m)	1037	526	1898	1168	423

3.2 Environmental Data and Prediction of Wind and Current Forces

The study was conducted using a water depth of 1829m considering 100-year hurricane conditions of the Gulf of Mexico. The JONSWAP wave spectrum having a significant wave height of 12.19m and a peak period of 14 seconds acting at 180 degrees was used as illustrated in Figure 6. The wind loading was generated using the Norwegian Petroleum Directorate (NPD) spectrum at 150degrees with a mean velocity of 41.12m/sec acting at 10m height. In addition, a current profile with a varying velocity of 0.941m/s to 0.0941m/sec from mean sea level to the sea bed is used[24].

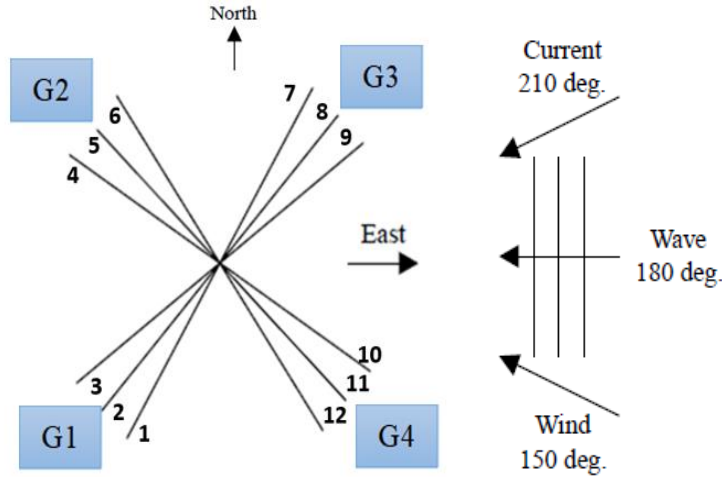


Figure 6: Illustration of the wave, wind, and current directions

3.3 Functionality of RegPSO

To determine the functionality of the RegPSO component of the tool, the RegPSO algorithm is validated using seven mathematical benchmark functions, including Ackley, the Griewangk, Quadric, Quartic Noise, Rastrigin, Rosenbrock, and weighted sphere as detailed in Table 3. These benchmarks were tested based on a varying number of particles and iterations. In each case, the problem dimension was maintained as 10, with a maximum of 30 particles at 250 iterations. The percentage of range to which each dimension is to be clamped (i.e., velocity clamping) is

350 maintained at 15% as recommended by Liu et al.,[25] because it performs better than the traditional
 351 50%.

352 Table 3: Benchmark Functions

Benchmarks	Function	Initial range of x_j
Ackley	$f(\vec{x}) = 20 + e - 20e^{-0.2\sqrt{\frac{\sum_{j=1}^n x_j^2}{n}}} - e^{\frac{\sum_{j=1}^n \cos(2x_j\pi)}{n}}$	$-32 \leq x_j \leq 32$
Griewangk	$f(\vec{x}) = 1 + \sum_{j=1}^n \frac{x_j^2}{4000} \prod_{j=1}^n \cos\left(\frac{x_j}{\sqrt{j}}\right)$	$-600 \leq x_j \leq 600$
Quadric	$f(\vec{x}) = \sum_{j=1}^n \left(\sum_{j=1}^n j \cdot x_j \right)^2$	$-100 \leq x_j \leq 100$
Quartic Noise	$f(\vec{x}) = \text{random}(0,1) + \sum_{j=1}^n j \cdot x_j^4$	$-1.28 \leq x_j \leq 1.28$
Rastrigin	$f(\vec{x}) = 10n + \sum_{j=1}^n (x_j^2 - 10\cos(2x_j\pi))$	$-5.12 \leq x_j \leq 5.12$
Rosenbrock	$f(\vec{x}) = \sum_{j=1}^{n-1} (100(x_{j+1} + x_j^2)^2 + (x_j)^2)$	$-30 \leq x_j \leq 30$
Weighted Sphere	$f(\vec{x}) = \sum_{j=1}^n j \cdot x_j^2$	$-5.12 \leq x_j \leq 5.12$

353
 354 These functions are selected to test the computational capability of the RegPSO algorithm to
 355 optimize both uni-modal and multimodal functions. For example, Ackley, Rastrigin, and
 356 Rosenbrock's functions are multi-modal while weighted sphere and the Griewangk's functions are
 357 unimodal. In each case, the existence of local minima tends to increase with increasing problem
 358 dimensionality. In this case, considering the mooring line design variables are less than 10, so we
 359 maintain a maximum dimension of 10 to test the capability by varying the number of particles and
 360 iterations. For each function, two trial was conducted to allow for average comparison.

3.4 Implementation of the Optimisation Procedure

363 The tool utilises an updated OrcaFlex data file linked with the RegPSO code to automatically
 364 search and update mooring design variables taking advantage of the robust functionality of the
 365 software. The functionality of the tool is influenced by many parameters, including the number of
 366 particles, dimension of the problem, number of iterations and other parameters as listed in Table
 367 4. The number of particles particularly dictates the size of the swarm (i.e., swarm = no of particle

1
2
3
4
5
6
7
8
9
10
11
12
13
14
15
16
17
18
19
20
21
22
23
24
25
26
27
28
29
30
31
32
33
34
35
36
37
38
39
40
41
42
43
44
45
46
47
48
49
50
51
52
53
54
55
56
57
58
59
60
61
62
63
64
65

* dimension). However, although the larger the number of particles the greater the chances of finding a global minimum, this can also result in parallel random search and in that case increasing the computational time. A varying number of particles ranging from 10 - 50 have been reported as appropriate for different variants of PSO [26]. On the other hand, the number of iterations together with the specified success threshold dictate the stopping criteria.

For each mooring variable, a range and central (median) value is defined to guide the search of the protocol to the global best.

Table 4: RegPSO parameter setting

Parameter	Value
Number of particles	Up to 10
Dimension of problem	6 and 7
Stagnation threshold	1.1×10^{-4}
Regrouping factor	1.2/ Stagnation threshold
Inertia weight	[0.9,0.4]
Max velocity clamping %	0.15
No. of iterations per group	varied
Max iteration overall grouping	varied

3.5 Integrated Design Methodology

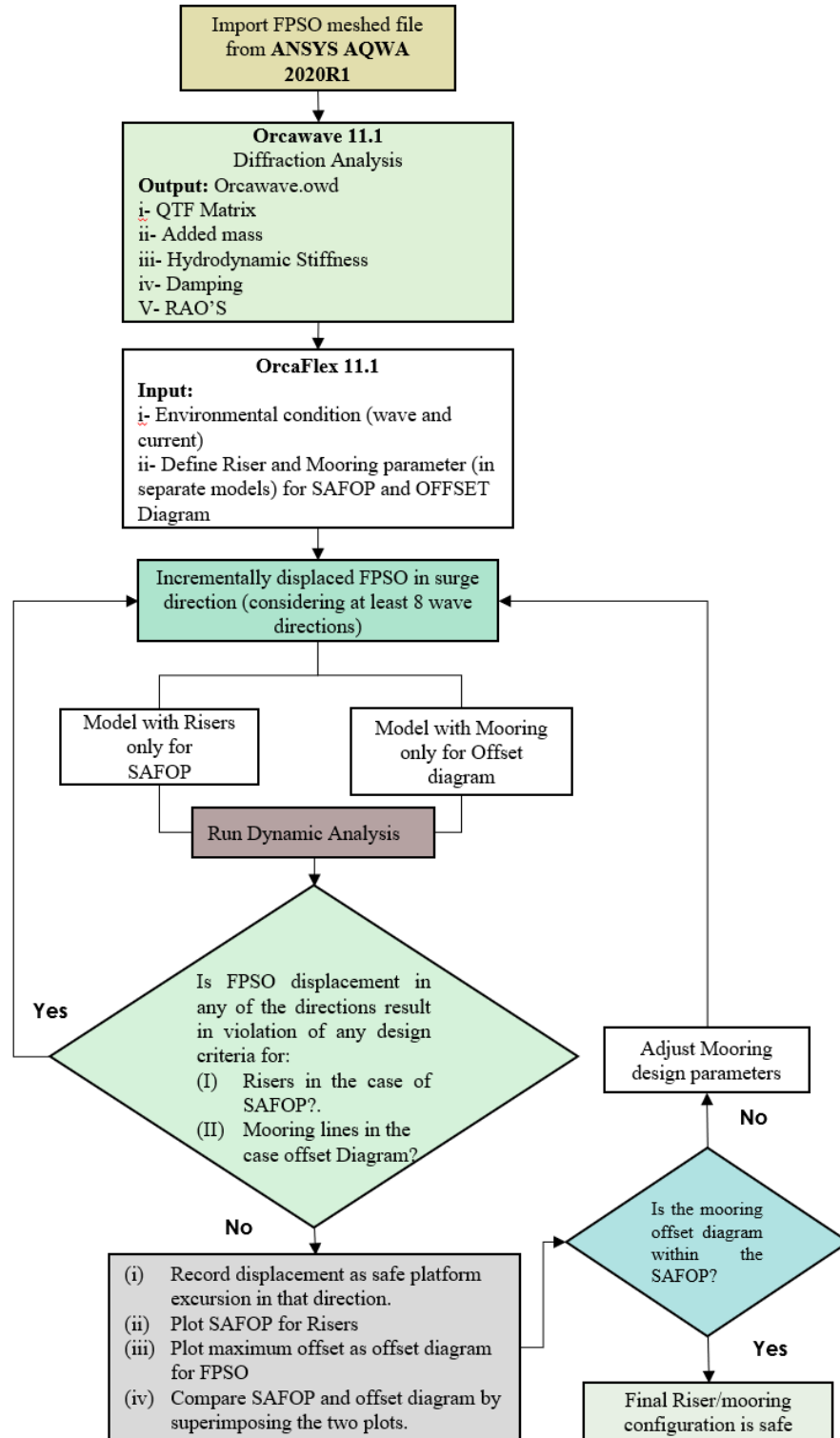
Previously, some of the few available mooring optimisation procedures considered only the mooring lines for the prediction of optimal platform offset without due consideration to the integrity of the risers [3, 4]. In this study, we incorporated the integrated design methodology which is implemented based on the flow chart illustrated in Figure 7. The procedure of producing SAFOP and offset diagrams.

The SAFOP is a polar diagram defining the horizontal displacement within which the top and the bottom connection point of the risers must remain to ensure none of the risers exceeds any of its design criteria in any of the wave directions considered. Here, we considered the 8 wave directions in producing the diagrams.

The offset diagrams on the hand are also polar diagrams that define the expected maximum horizontal excursions of the floater.

The superposition of the two diagrams gives a visual verification/assessment of the design criteria for the riser and mooring lines.

1
2
3
4
5
6
7
8
9
10
11
12
13
14
15
16
17
18
19
20
21
22
23
24
25
26
27
28
29
30
31
32
33
34
35
36
37
38
39
40
41
42
43
44
45
46
47
48
49
50
51
52
53
54
55
56
57
58
59
60
61
62
63
64
65



392
393 Figure 7: Flow chart for implementation of Safe Operation Zone (SAFOP) and offset Diagram for the
394 Mooring system

4 Results and Discussions

4.1 Validation of FPSO model for hydrodynamic data

The validation results (AQWA) consisting of static offset, free decay, and hydrodynamic response results in six degrees of freedom (6DOF) degrees well with the published results [3] as shown in Figure 6, Tables 5 and 6 respectively. Figure 8 compares the mooring restoring forces from both models, which tend to linearly increase with increasing platform excursion. However, a slight variation of 3% between the WINPOST and AQWA model is observed at about 80m to 90m excursions.

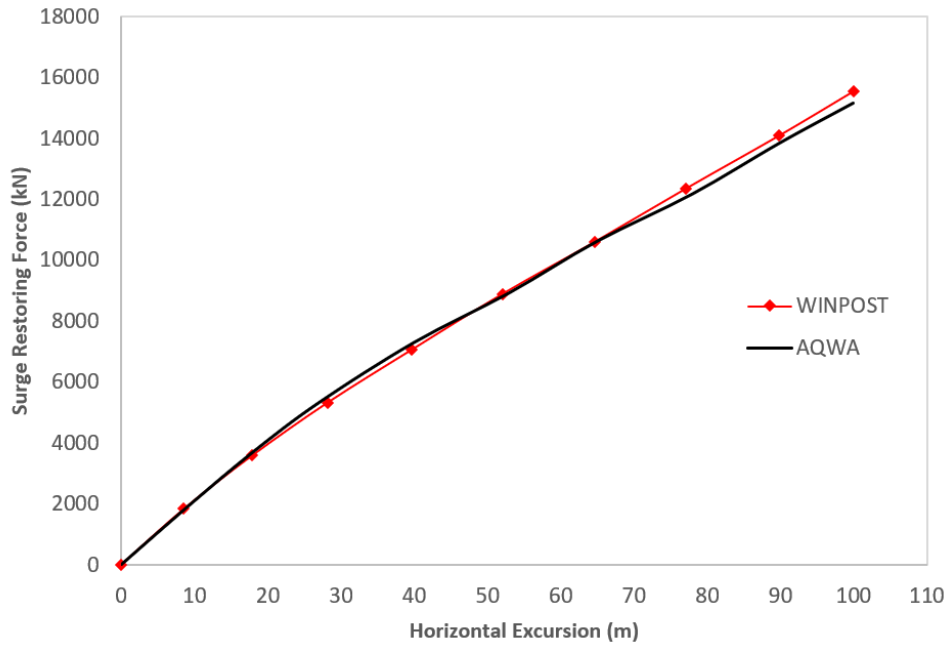


Figure 8: Comparison of Restoring Behaviour of the WINPOST and AQWA model

From Table 5, the natural periods of the AQWA model for all the degrees of freedom considered are within the range of both published experimental and simulation results. The same trend is observed in the case of the damping ratios, with the AQWA model having damping ratios closer to the published experimental results. Overall, the results compare well with the published restoring force, natural periods, and damping ratios.

Table 5: Comparisons of Validation free decay results

	Periods(sec)			Damping (%)		
	AQWA	WINPOST	OTRC	AQWA	WINPOST	OTRC
Surge	205.2	204.7	206.8	3.7	4.4	3.0
Heave	10.8	10.8	10.7	4.5	11.8	6.7
Roll	12.7	12.7	12.7	3.2	0.7	3.4
Pitch	10.7	10.8	10.5	7.5	10.5	8.0

Table 6 statistically compares the responses of the AQWA model in 6DOF with the published results. This reveals close agreement with the published results, thereby proving the accuracy adopted in the validation process.

Table 6: Comparison of validation results in 6DOF

	Source	Surge(m)	Sway(m)	Heave(m)	Roll (deg)	Pitch (deg)	Yaw (deg)
Max	AQWA	4.44	11.2	8.33	8.2	3.37	-15.21
	WINPOST	2.29	13.1	10.9	3.5	4.45	-3.4
	OTRC	6.30	10.9	9.11	9.57	4.2	-8.69
Min	AQWA	-60.22	-20.04	-10.45	-7.26	-4.37	-29.72
	WINPOST	-61.30	-21.4	-11.3	-3.6	-4.99	-24.6
	OTRC	-54.10	-13.6	-9.52	-8.77	-4.07	-23.3
Mean	AQWA	-20.77	-0.48	0.11	0.06	0.17	-18.37
	WINPOST	-22.90	-0.09	0.14	-0.1	0.01	-16
	OTRC	-21.10	-0.64	-0.06	-0.08	0.03	-16.8
SD	AQWA	7.97	4.55	2.92	1.45	1.19	5.03
	WINPOST	9.72	4.57	3.08	0.9	1.31	3.8
	OTRC	8.78	4.05	2.81	2.18	1.26	2.46

4.2 The Functionality of the RegPSO Algorithm

Table 7 shows the statistical performance of RegPSO code in optimising various mathematical benchmark functions with a different number of particles. It can be observed that with an increasing number of particles the global minima also decrease. This is due to the consequent increase in swarm size which increases the number of possible solutions. Thus, this indicates the capability of the RegPSO in finding the optimum solution for the selected mathematical benchmark functions.

For the mean of the two trials conducted for each benchmark, it can be observed that the code has successfully minimised Ackley function by 99%, the Griewangk function by 90%, Quadric by 99.9% and Quartic Noisy by 96.1%. The code also minimises Rastrigin by 82%, Rosenbrock by 98% and weighted sphere by 100%. The Rastrigin benchmark function result is particularly impressive because the benchmark generally returns high function values due to the stagnation of the swarm.

Table 8 shows the statistical comparison of RegPSO performance across seven benchmark functions with an increasing number of iterations. A similar trend was observed in Table 7. The code was able to minimise the Ackley function by 97%, the Griewangk function by 72%, the Quadric function by 99% and Quartic Noisy by 80%. It has also minimised the Rastrigin function by 56%, Rosenbrock function by 58% and weighted sphere by 99%.

Table 7: Functionality of RegPSO across Mathematical benchmarks with different numbers of particles

Benchmark functions	Dimension	No. particle		Number of particles		
				2	10	30
Ackley	10	30	Mean	6.6583	0.16809	0.07034
			min	4.519	0.11141	0.05609
			max	8.7979	0.22476	0.08459
			std	3.0254	0.08015	0.02015
Griewangk	10	30	Mean	1.9885	0.46766	0.19584
			min	1.5313	0.36529	0.12548
			max	2.4458	0.57004	0.2662
			std	0.64665	0.14478	0.0995
Quadric	10	30	Mean	1397.62	4.3421	0.87772
			min	616.936	1.9549	0.23309
			max	2178.3	6.7294	1.5223
			std	1104.05	3.3761	0.91165
Quartic Noisy	10	30	Mean	0.14832	0.01337	0.00578
			min	0.13059	0.00732	0.0047
			max	0.16605	0.01942	0.00685
			std	0.02507	0.00856	0.00152
Rastrigin	10	30	Mean	41.6264	14.8883	7.5733
			min	38.5929	4.8645	7.1779
			max	44.6599	24.9121	7.9686
			std	4.29	14.1758	0.55905
Rosenbrock	10	30	Mean	4344.47	367.807	85.7507
			min	3761.15	207.586	72.4246
			max	4927.79	528.027	99.0768
			std	824.941	226.586	18.8459
weighted Sphere	10	30	mean	2.8269	0.00045	0.00028
			min	1.1083	0.00034	0.00028
			max	4.5455	0.00055	0.00029
			std	2.4305	0.00015	1.31E-05

446
447

Table 8: Functionality of RegPSO across Mathematical benchmarks with different iteration numbers

Benchmark	Dimension	No. particle		No. of iterations					
				50	100	150	200	250	800
Ackley	10	30	Mean	2.0427	0.69939	0.14082	0.09578	0.0703	4.6915E-6
			min	1.9482	0.63282	0.11526	0.06006	0.0560	1.606E-7
			max	2.1371	0.76596	0.16637	0.13151	0.0845	8.7023E-9
			std	0.13359	0.09414	0.03614	0.05051	0.0201	1.4519E-7
Griewangk	10	30	Mean	0.70807	0.52323	0.32358	0.27586	0.1958	0.009857
			min	0.62384	0.41003	0.2449	0.18308	0.1254	0.013861
			max	0.7923	0.63643	0.40226	0.36864	0.2662	0.058867
			std	0.11912	0.16009	0.11127	0.13121	0.0995	0.01552
Quadric	10	30	Mean	118.925	16.5321	3.9363	1.9285	0.8777	3.1351E-4
			min	54.6702	16.1066	2.9926	0.77378	0.2330	6.0537E-9
			max	183.180	16.9576	4.8799	3.0832	1.5223	9.5804E-5
			std	90.8706	0.60178	1.3345	1.633	0.9116	2.2243E-10
Quartic Noisy	10	30	Mean	0.02952	0.01595	0.01309	0.00740	0.0057	5.7801E-2
			min	0.02867	0.01401	0.01217	0.00685	0.0047	
			max	0.03036	0.01789	0.01401	0.00795	0.0068	
			std	0.00119	0.00274	0.0013	0.00077	0.0015	
Rastrigin	10	30	Mean	17.0199	8.2907	7.9991	7.9822	7.5733	2.6824E-11
			min	13.2245	8.256	7.9812	7.9753	7.1779	0
			max	20.8152	8.3254	8.017	7.9892	7.9686	1.3337E-9
			std	5.3675	0.04908	0.02533	0.00982	0.5590	1.886E-10
Rosenbrock	10	30	Mean	206.476	108.674	88.7519	88.0642	85.750	0.003935
			min	190.928	104.681	78.4269	77.0515	72.424	1.7028E-6
			max	222.025	112.667	99.0768	99.0768	99.076	0.018039

			std	21.9886	5.6469	14.6017	15.5742	18.845	0.004137	
								9	5	
	Weighted	10	30	mean	0.02652	0.00472	0.00062	0.00051	0.0002	9.8177E-
	Sphere				5	9	6	8	8	14
				min	0.02249	0.00105	0.0006	0.00051	0.0002	1.9112E-
					3			8	14	
				max	0.03055	0.00840	0.00065	0.00052	0.0002	2.5244E-
					7	7	5	6	9	13
				std	0.00570	0.00520	4.09E-	1.13E-	1.3E-	5.4364E-
					2	2	05	05	05	14

Observing Tables 7 and 8, it is clear to notice the drop in values with an increasing number of particles and number of iterations respectively for all the benchmarks. This indicates the capability of the code to minimise the seven mathematical benchmark functions consisting of uni, bi and multi-modal functions by explicitly exploring and exploiting the search space. It is also interesting to observe the consistency of the code across all the benchmarks considered.

4.3 Case studies of Optimization Problems

To demonstrate the functionality of the Optimisation tool (MooOpT4FPSO), two case studies considering the validated model described in section 3 were used to optimise the mooring line parameters of the turret FPSO with 4x3 and 3x3 configurations with 12 and 9 mooring lines.

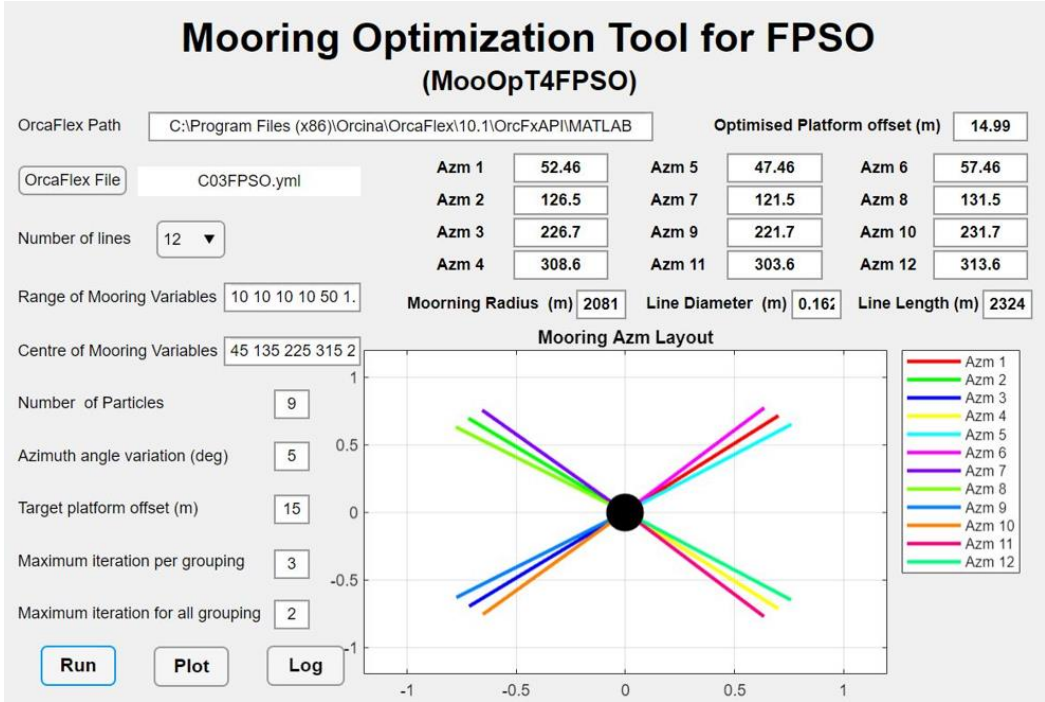
4.3.1 Case of Turret FPSO with Twelve Taut Mooring Lines

Figure 9 illustrates the optimization results from MooOpT4FPSO for turret FPSO with 12 lines. The GUI illustrate the optimised parameters to maintain a platform of 15m and a mooring azimuth layout.

Furthermore, Tables 9 and 10 illustrate the optimal solutions for the mooring design variables.

Table 9 shows the comparison of original and optimised mooring line azimuth angles. Other parameters presented are shown in Table 10. Which shows the reduction in line length and diameter and mooring radius, with a consequent reduction in platform offset from 40.8m to 14.99m as specified (target platform offset). This is equivalent to a 63.3% reduction in the platform offset. In addition, the reduction in line length and diameter comes with a reduction in line material and resulting payload. Also, a reduction in mooring radius will yield a consequent reduction in line tension.

1
2
3
4
5
6
7
8
9
10
11
12
13
14
15
16
17
18
19
20
21
22
23
24
25
26
27
28
29
30
31
32
33
34
35
36
37
38
39
40
41
42
43
44
45
46
47
48
49
50
51
52
53
54
55
56
57
58
59
60
61
62
63
64
65



471
472 Figure 9: Complete optimization result for turret FPSO with 12 mooring line

473
474 Table 9: Comparison of original and Optimised mooring Azimuth angles

Line	Azimuth (°)	
	Original	Optimized
Line 1	45	52.46
Line 2	135	126.5
Line 3	225	226.7
Line 4	315	308.6
Line 5	40	47.46
Line 6	50	57.46
Line 7	130	121.5
Line 8	140	131.5
Line 9	220	221.7
Line10	230	231.7
Line11	310	303.6
Line12	320	313.6

475
476
477 Table 10: Comparison of original and Optimized Mooring length, line diameter and Mooring radius

	Original	Optimized	%Difference
Mooring Length (m)	2438	2324	4.7
Diameter(mm)	170	162	4.7
Mooring Radius(m)	2090	2081	0.43
Surge Offset	40.8	14.99	63.3

4.3.2 Case of Turret FPSO with Nine Taut Mooring Lines

In the case of turret moored FPSO with 9 mooring lines, the 4th row of azimuth angles consisting of lines #4, #11 and #12 as shown in the GUI are not considered as shown in Figure 10. Tables 10 and 11 compares original and optimized line parameters from MooOpT4FPSO. In each case, the optimized parameters are better than the original in terms of reduction in line length and diameter.

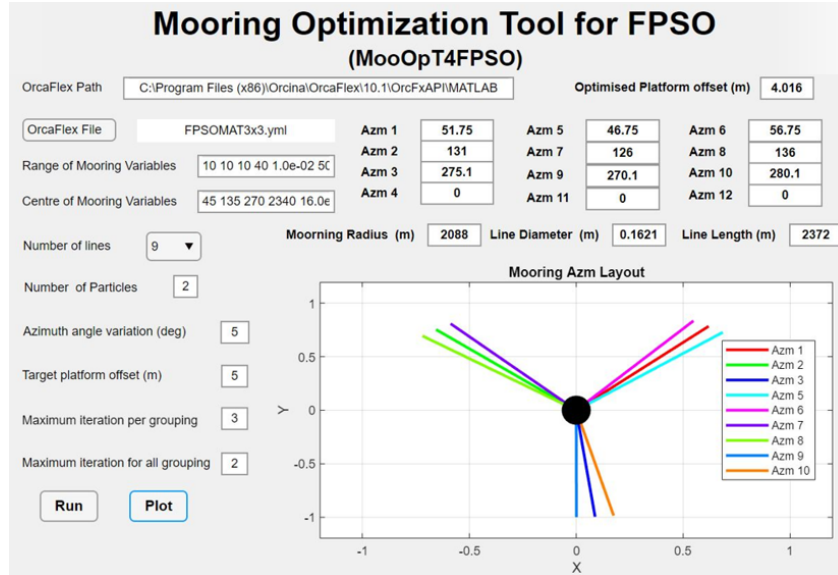


Figure 10: Complete optimization result for turret FPSO with 9 mooring lines

Table 11: Comparison of original and Optimised mooring Azimuth angles

Line	Azimuth (°)	
	Original	Optimized
Line 1	50	51.75
Line 2	135	131
Line 3	270	275.1
Line 4	45	46.75
Line 5	55	56.75
Line 6	130	126
Line 7	140	136
Line 8	265	270.1
Line 9	270	280.1

Table 12: Comparison of original and Optimized Mooring length, line diameter and Mooring radius

	Original	Optimized	%Difference
Mooring Length (m)	2438	2372	3
Diameter(mm)	170	162.1	4.6
Mooring Radius(m)	2090	2088	0.1
Surge Offset	44.2	23.21	47.5

4.3.3 Case of Turret FPSO with Twelve Catenary Mooring Lines

The optimization result for a turret FPSO with 12 catenary mooring lines is illustrated in Figure 11. The results indicated optimized mooring parameters required to maintain the platform within a 30-meter offset as defined during the analysis. Detailed comparisons are presented in Tables 13 and 14.

Table 13 compares the mooring line azimuth angle of the original and optimized models. On the other hand, Table 14 compares the mooring line length, mooring radius, and line diameter of the original and optimised model. In each case, the optimised parameters present better line parameters, with the 3.4%, 5.2% and 2.8% reduction in mooring line length, diameter, and mooring radius, respectively on every single line. In addition, a significant reduction in platform offset of 67.7% was recorded. The optimised result is consistent with the ones presented for taut moorings thereby confirming the capability of the tool.

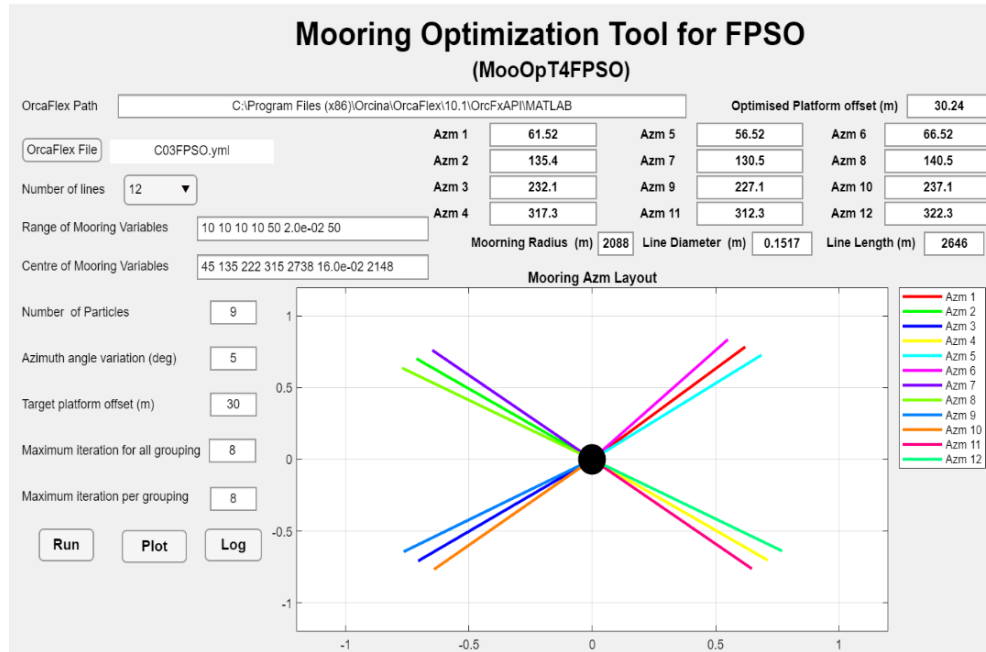


Figure 11: Complete Optimization result for turret FPSO with 12 Catenary mooring lines

Table 13: Comparison of original and Optimized mooring Azimuth angles

Line	Azimuth (°)	
	Original	Optimized
Line 1	45	61.52
Line 2	135	135.4
Line 3	225	232.1
Line 4	315	317.0
Line 5	40	56.53

Line 6	50	66.52
Line 7	130	130.4
Line 8	140	140.4
Line 9	220	227.1
Line10	230	237.1
Line11	310	312.0
Line12	320	322.0

Table 14: Comparison of original and Optimized Mooring length, line diameter and Mooring radius

	Original	Optimized	%Difference
Mooring Length (m)	2738	2646	3.4
Diameter(mm)	160	151.7	5.2
Mooring Radius(m)	2148	2088	2.8
Surge Offset	93.4	30.2	67.7

4.3.4 Case of Turret FPSO with Nine Catenary Mooring Lines

Figure 12 illustrates optimised results of turret FPSO with 9 catenary mooring lines from MooOpT4FPSO.

The detail of the results is further elaborated in Tables 15 and 16. The variations of azimuth angles as illustrated in Table 15 has a direct influence on mooring line length, diameter and the mooring radius as shown in Table 16. Most importantly the resulting optimised line parameters have successfully reduced the platform offset by 64.5%.

This is consistent with the results obtained by other mooring configurations presented using taut moorings.

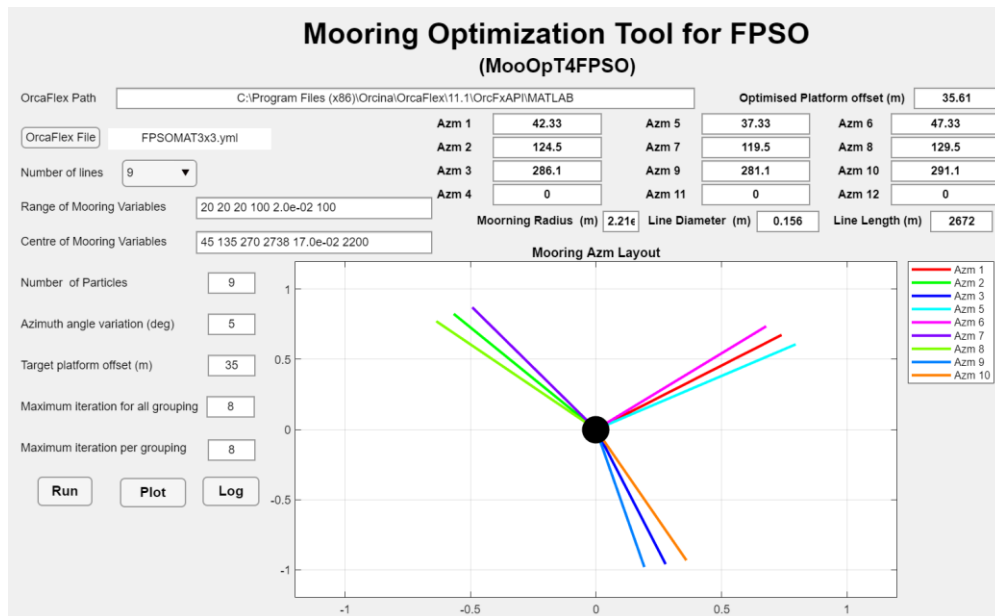


Figure 12: Complete Optimization result for turret FPSO with 9 Catenary mooring lines

Table 15: Comparison of original and Optimised mooring Azimuth angles

Line	Azimuth (°)	
	Original	Optimized
Line 1	50	42.33
Line 2	135	124.45
Line 3	270	286.10
Line 4	45	37.33
Line 5	55	47.33
Line 6	130	119.45
Line 7	140	129.45
Line 8	265	281.1
Line 9	270	291.1

Table 16: Comparison of original and Optimized Mooring length, line diameter and Mooring radius

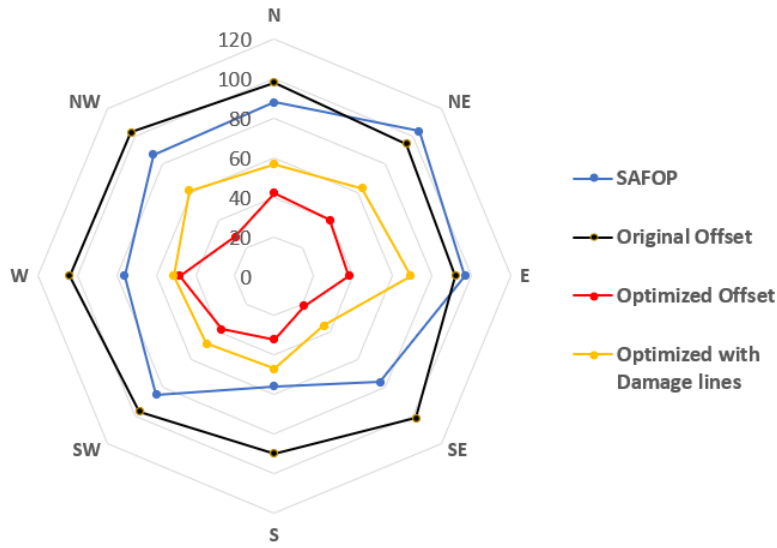
	Original	Optimized	%Difference
Mooring Length (m)	2738	2672	2.40
Diameter(mm)	160	156.1	2.40
Mooring Radius(m)	2148	2096	2.42
Surge Offset	100.2	35.6	64.5

4.4 Evaluation of Optimized Mooring Offset with riser SAFOP in intact and Damage Conditions.

4.4.1 Comparison with FPSO with Twelve Taut Mooring Lines

The superimposed SAFOP and offset diagram in Figure 13 compare the maximum offset of the original model with 12 taut lines and optimized mooring configurations (intact and damaged) with the SAFOP limits to ensure the integrity of the risers in all 8 directions considered. From these figures, it can be observed that the optimized mooring configurations maintain the platform within the SAFOP zone of the risers even in the event of a line failure.

1
2
3
4 541
5
6
7
8
9
10
11
12
13
14
15
16
17
18
19
20
21
22



23 542
24
25 543
26 544
27

Figure 13: Comparison of SAFOP and Optimised offset diagrams for FPSO with 12 mooring lines with damaged lines.

28 545 4.4.2 Comparison with Turret FPSO with Nine Taut Mooring Lines

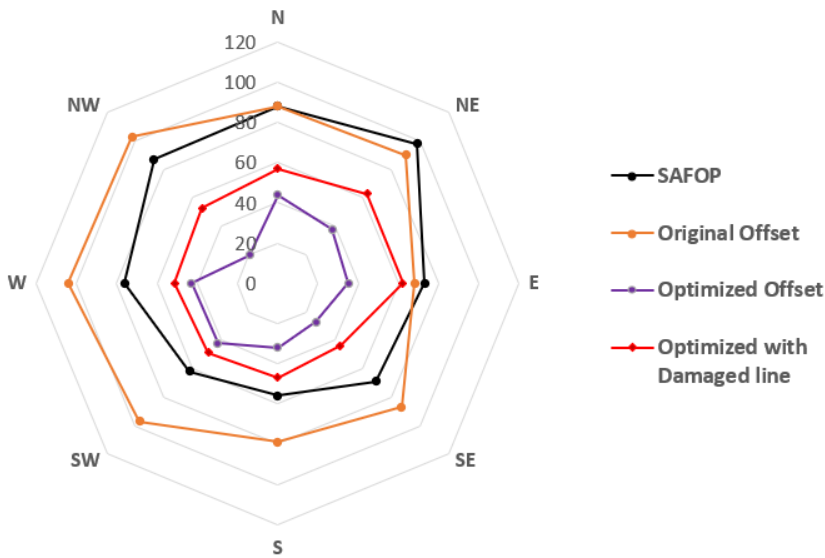
29
30 546
31
32 547

Figures 14 compares the platform offset of the original FPSO with nine taut moorings, the optimised (intact and damaged) with the SAFOP.

33
34 548
35
36 549
37 550

It can be observed for both intact and damaged conditions, the optimised platform offsets in all directions are maintained within the riser SAFOP. While for the original model, platform offset is only maintained in two directions (NE and E).

38
39
40
41
42
43
44
45
46
47
48
49
50
51
52
53
54
55



56 551
57
58 552
59 553
60
61
62
63
64
65

Figure 14: Comparison of SAFOP and Optimized offset diagrams for FPSO with 9 mooring lines with damaged lines.

1
2
3
4
5
6
7
8
9
10
11
12
13
14
15
16
17
18
19
20
21
22
23
24
25
26
27
28
29
30
31
32
33
34
35
36
37
38
39
40
41
42
43
44
45
46
47
48
49
50
51
52
53
54
55
56
57
58
59
60
61
62
63
64
65

4.4.3 Comparison with Turret FPSO with Twelve Catenary Mooring Lines

Figures 15 illustrate the comparison of platform offset for the original and optimised model from MooOpT4FPSO. This case considers catenary mooring lines in intact and damaged condition.

The optimized platform offset can be observed to be within the SAFOP in all 8 directions while the platform offset from the original model can be seen to go beyond the SAFOP in 4 directions (NW, W, SW, S).

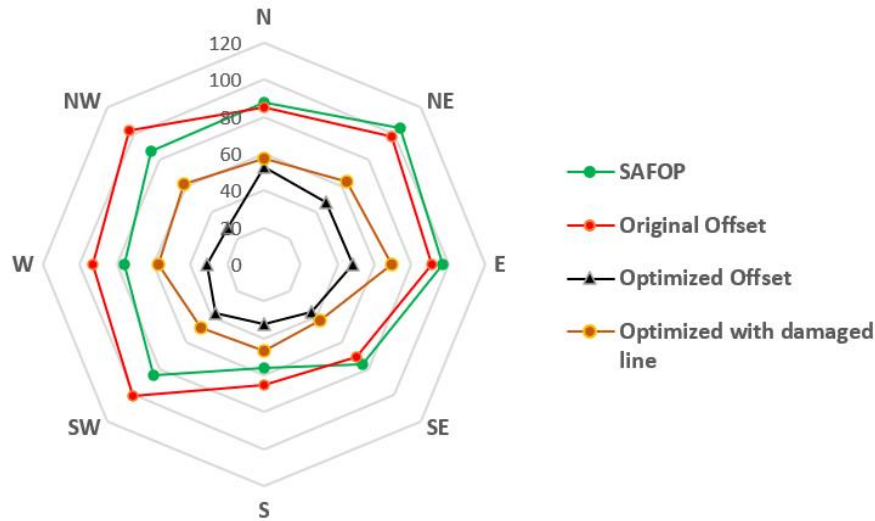


Figure 15: Comparison of SAFOP and Optimised offset diagrams for FPSO with 12 catenary mooring lines with a damaged line.

4.4.4 Comparison with Turret FPSO with Nine Catenary Mooring Lines

In this case, Figure 16 compare the platform offset of turret FPSO with 9 catenary lines.

Similar to what was observed in Figure 15, the optimised offset can be observed to be within the SAFOP in all 8 directions compared to the original. Also, in the case of damage, the optimised offset is maintained within the riser SAFOP.

This infers the efficiency of the tool in providing mooring parameters that ensure platform offset is maintained within the risers' safe operation zones.

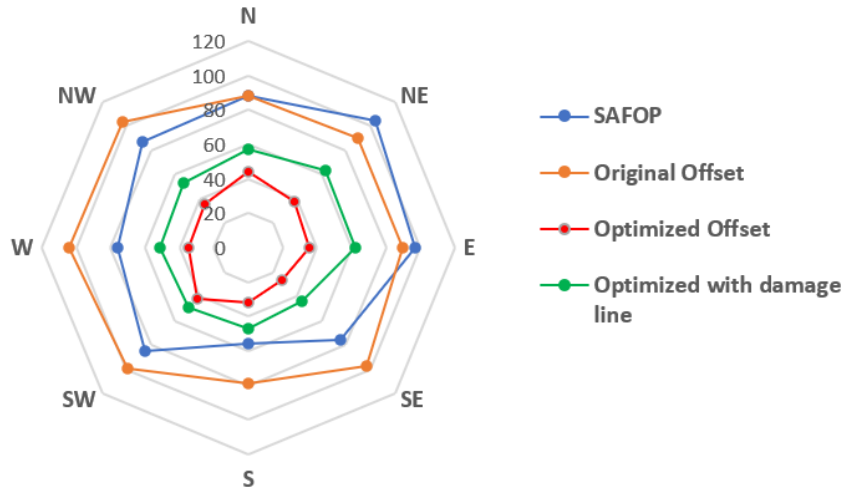


Figure 16: Comparison of SAFOP and Offset diagrams for FPSO with 9 Catenary mooring lines

5 Conclusion

In this paper, we presented an optimisation procedure of mooring line parameters for a turret moored FPSO using a Mooring Optimisation Tool for FPSO (MooOpT4FPSO). The tool is an integration of the Regrouping particle swarm optimisation (RegPSO) algorithm and a commercial software OrcaFlex. In addition, the integrated riser-mooring design methodology has been incorporated to take into consideration the interaction of the riser, mooring and the FPSO hull. The superimposed riser safe operation zone (SAFOP) and the platform offset diagram are used to assess and ensure that maximum platform offset is maintained within the riser safe operating zone. The specific conclusion from this study are as follows:

- 1) The Optimization tool has successfully simultaneously optimized mooring line length (mid-segment), line diameter, mooring radius, and azimuth angles of turret FPSO while ensuring platform excursions are maintained within the riser safe operation zone, which is very important.
- 2) The tool has the computational capability of optimizing mooring line parameters of turret FPSO with 12 and 9 mooring lines to achieve target platform offset.
- 3) From the optimised results, the application of the tool in mooring design can bring a reduction in line material and consequently the overall project cost, in addition to the reduction of payload exerted on the platform.

Acknowledgements

The authors acknowledged the Universiti Teknologi PETRONAS, Malaysia for supporting this research under YUTP 015LC0-116.

1
2
3
4
5
6
7
8
9
10
11
12
13
14
15
16
17
18
19
20
21
22
23
24
25
26
27
28
29
30
31
32
33
34
35
36
37
38
39
40
41
42
43
44
45
46
47
48
49
50
51
52
53
54
55
56
57
58
59
60
61
62
63
64
65

598 References

- [1] I. A. Ja'e, M. O. A. Ali, A. Yenduri, Z. Nizamani, and A. Nakayama, "Optimisation of mooring line parameters for offshore floating structures: A review paper," *Ocean Engineering*, vol. 247, p. 110644, 2022.
- [2] B. da Fonseca Monteiro, J. S. Baioco, C. H. Albrecht, B. S. L. P. de Lima, and B. P. Jacob, "Optimization of mooring systems in the context of an integrated design methodology," *Marine Structures*, vol. 75, p. 102874, 2021.
- [3] O. Montasir, A. Yenduri, and V. Kurian, "Mooring system optimisation and effect of different line design variables on motions of truss spar platforms in intact and damaged conditions," *China Ocean Engineering*, vol. 33, no. 4, pp. 385-397, 2019.
- [4] S. F. Senra, F. N. Correa, B. P. Jacob, M. r. M. Mourelle, and I. a. Q. Masetti, "Towards the Integration of Analysis and Design of Mooring Systems and Risers: Part I—Studies on a Semisubmersible Platform," in *International Conference on Offshore Mechanics and Arctic Engineering*, 2002, vol. 36118, pp. 41-48.
- [5] S. Mehdi and A. Rezvani, "Mooring optimization of floating platforms using a genetic algorithm," *Ocean Engineering*, vol. 34, no. 10, pp. 1413-1421, 2007, doi: 10.1016/j.oceaneng.2006.10.005.
- [6] S. A. R. D. S. Maffra, M. A. C. Pacheco, and I. F. M. g. de Menezes, 1, 3., "Genetic Algorithm Optimization for Mooring Systems," *Generations*, vol. 1, no. 3, 2003.
- [7] J. J. C. Alonso, F. M. M. Ivan, and F. M. Luiz, "Mooring Pattern Optimization using Genetic Algorithms " in *6th World Congresses of Structural and Multidisciplinary Optimization*, Rio de Janeiro, Brazil, 2005, pp. 1-9.
- [8] M. Liang, X. Wang, S. Xu, and A. Ding, "A shallow water mooring system design methodology combining NSGA-II with the vessel-mooring coupled model," *Ocean Engineering*, vol. 190, Oct 15 2019, Art no. 106417, doi: 10.1016/j.oceaneng.2019.106417.
- [9] B. da Fonseca Monteiro, C. H. Albrecht, and B. P. Jacob, "Application of the particle swarm optimization method on the optimization of mooring systems for offshore oil exploitation," in *Proceedings of Second International Conference on Engineering Optimization*, 2010.
- [10] B. Da Fonseca Monteiro, M. H. A. De Lima Jr, C. H. Albrecht, B. De Souza Leite, P. De Lima, and B. P. Jacob, "Mooring optimization of offshore floating systems using an improved particle swarm optimization method," 2013, vol. 1, doi: 10.1115/OMAE2013-11096. [Online]. Available:
- [11] B. D. F. Monteiro, J. S. Baioco, C. H. Albrecht, B. S. L. P. de Lima, and B. P. Jacob, "Optimization of mooring systems in the context of an integrated design methodology," *Marine Structures*, Article vol. 75, 2021, Art no. 102874, doi: 10.1016/j.marstruc.2020.102874.
- [12] B. F. Monteiro, A. A. de Pina, J. S. Baioco, C. H. Albrecht, B. S. L. P. de Lima, and B. P. Jacob, "Toward a methodology for the optimal design of mooring systems for floating offshore platforms using evolutionary algorithms," *Marine Systems and Ocean Technology*, Article vol. 11, no. 3-4, pp. 55-67, 2016, doi: 10.1007/s40868-016-0017-8.
- [13] *Analysis of Stationkeeping Systems for Floating Structures*, A. Design, 2005.
- [14] A. R. C. Girón, F. N. Corrêa, A. O. V. Hernández, and B. P. Jacob, "An integrated methodology for the design of mooring systems and risers," *Marine Structures*, vol. 39, pp. 395-423, 2014.
- [15] B. Seymour, H. Zhang, and C. Wibner, "Integrated Riser and Mooring design for the P-43 and P-48 FPSOs," in *Offshore Technology Conference*, 2003: Offshore Technology Conference.
- [16] *Offshore Standard: Position Mooring*, D. N. Veritas, 2010.
- [17] P. Chakrabarti, R. Chandwani, and I. Larsen, "Analyzing the effect of integrating riser/mooring line design," in *Proceedings of OMAE*, 1996: American Society of Mechanical Engineers, New York, NY (United States).

1
2
3
4
5
6
7
8
9
10
11
12
13
14
15
16
17
18
19
20
21
22
23
24
25
26
27
28
29
30
31
32
33
34
35
36
37
38
39
40
41
42
43
44
45
46
47
48
49
50
51
52
53
54
55
56
57
58
59
60
61
62
63
64
65

[18] D. Garrett, J. Chappell, R. Gordon, and Y. Cao, "Integrated Design of Risers and Moorings," in *Deepwater Mooring Systems: Concepts, Design, Analysis, and Materials*, 2003, pp. 300-315.

[19] F. c. N. Correa, S. F. Senra, B. P. Jacob, I. a. Q. Masetti, and M. r. M. Mourelle, "Towards the Integration of Analysis and Design of Mooring Systems and Risers: Part II—Studies on a DICAS System," in *International Conference on Offshore Mechanics and Arctic Engineering*, 2002, vol. 36118, pp. 291-298.

[20] *Design and Analysis of Stationkeeping Systems for Floating Structures*, API, Washington DC, 2005.

[21] George I. Evers and M. B. Ghalia, "Regrouping Particle Swarm Optimization:A New Global Optimization Algorithm with Improved Performance Consistency Across Benchmarks," in *IEEE International Conference on Systems, Man, and Cybernetics*, San Antonio, TX, USA, 2009, pp. 3901-3908.

[22] M. Kaucic, "A multi-start opposition-based particle swarm optimization algorithm with adaptive velocity for bound constrained global optimization," *Journal of Global Optimization*, vol. 55, no. 1, pp. 165-188, 2013.

[23] F. Van Den Bergh, "An analysis of particle swarm optimizers," University of Pretoria, 2007.

[24] M. Kim, B. Koo, R. Mercier, and E. Ward, "Vessel/mooring/riser coupled dynamic analysis of a turret-moored FPSO compared with OTRC experiment," *Ocean Engineering*, vol. 32, no. 14-15, pp. 1780-1802, 2005.

[25] B. Liu, L. Wang, Y.-H. Jin, F. Tang, and D.-X. Huang, "Improved particle swarm optimization combined with chaos," *Chaos, Solitons & Fractals*, vol. 25, no. 5, pp. 1261-1271, 2005.

[26] A. P. Piotrowski, J. J. Napiorkowski, and A. E. Piotrowska, "Population size in particle swarm optimization," *Swarm and Evolutionary Computation*, vol. 58, p. 100718, 2020.

Optimization of Mooring Line Design Parameters Using Mooring Optimization Tool for FPSO (MooOpT4FPSO) with the Consideration of Integrated Design Methodology

Idris Ahmed Ja'e^{1,2}, Montasir Osman Ahmed Ali^{1,*}, Anurag Yenduri³, Chiemela Victor Amaechi^{4,5}, Zafarullah Nizamani⁶ and Akihiko Nakayama⁶

¹ Civil and Environmental Engineering Department, Universiti Teknologi PETRONAS, Bandar Seri Iskandar, Perak 32610, Malaysia. idris_18001528@utp.edu.my

² Department of Civil Engineering, Ahmadu Bello University, Zaria, Kaduna State, 810107, Nigeria

³ Global Engineering Centre, Subsea Engineering, TechnipFMC, India, 600032, Chennai, yendurianurag@gmail.com

⁴ Department of Engineering, Lancaster University, Lancaster, LA1 4YR, UK. c.amaechi@lancaster.ac.uk

⁵ Standards Organisation of Nigeria (SON), 52 Lome Crescent, Wuse Zone 7, Abuja, 900287, Nigeria

⁶ Department of Environmental Engineering, Universiti Tunku Abdul Rahman (UTAR), 31900, Kampar, Perak, Malaysia; zafarullah@utar.edu.my, akihiko@utar.edu.my

*Correspondence: montasir.ahmedali@utp.edu.my.

Abstract

Optimisation of mooring line design parameters including line azimuth angles, line diameter, line length and mooring radius is presented for a turret-moored FPSO. The optimisation procedure is implemented using a Mooring Optimisation Tool for FPSO (MooOpT4FPSO), which is an in-house optimisation tool purposely developed for this purpose. The tool is a synchronisation of the Regrouping Particle Swarm Optimisation (RegPSO) algorithm with commercial software, OrcaFlex. Case studies using a validated numerical FPSO model moored with multicomponent mooring lines acted upon by non-collinear wave, wind and current were analysed using the developed tool. To take into consideration the interaction of the riser system in the optimisation procedure, the integrated design methodology was adopted where the riser safe operation (SAFOP) zone diagram combined with the offset diagram is used for the verification/assessment of the design criteria of the risers and mooring lines. The optimized FPSO model offsets in eight directions are found to be within the riser safe operation zone. Based on the results, the tool was able to simultaneously optimise the mooring line diameter, line length, mooring radius, and azimuth angles of the turret FPSO to achieve a specific offset. Application of the tool can help the industry save material (by reduction of line diameter and length) and consequently the overall project cost, in addition to the reduction of structural payload exerted on the platform. Furthermore, the tool has an automatic search capability, which is an improvement to the conventional mooring design approach that is based on a trial-and-error approach.

1
2
3
4 34 **Keywords:** Optimization, Mooring line design parameters, FPSO, RegPSO, OrcaFlex, SAFOP
5

6
7 35 **1 Introduction**

8 36 Mooring system design entails consideration of several factors including the composition of the
9 37 mooring lines, type of platform to be moored, environmental conditions and the time the platform
10 38 will remain anchored in position. Dynamic positioning systems, tethers, mooring lines, or a
11 39 combination of both are used to maintain floating platforms in position. As a result, the mooring
12 40 system's ability to maintain the platform in place has a significant influence on the integrity of the
13 41 risers and the floating platform in general. Hence, the efficiency of the mooring system is largely
14 42 dictated by the mooring line design parameters, including mooring line material, line length,
15 43 azimuth angles, diameter, line pretension, mooring radius etc. However, the selection of these
16 44 design parameters in the currently available procedure is based on a trial-and-error/manual
17 45 approach which depends mainly on the experience of the engineer, thereby making it extremely
18 46 time-consuming[1-3]. In addition, the moorings and risers are designed separately with little
19 47 interaction between the two design teams and mostly using uncoupled analysis[2, 4]. The selection
20 48 of maximum platform offset in both intact and damaged conditions is also done arbitrarily
21 49 irrespective of the direction. The risers are subsequently designed to satisfy their functional
22 50 requirement by considering the same offset. This indicates the target offset values as the only
23 51 connection that links the mooring and riser designs[1].
24
25
26
27
28

29
30 52 Hence, the increased application of FPSOs in deeper waters necessitates the need for an optimum
31 53 mooring design that ensures minimum platform horizontal excursion during operation[5]. This is
32 54 important because substantial platform excursions place an enormous constraint on the workability
33 55 of offshore floating structures. Thus, an optimum mooring system can be achieved by automating
34 56 the search component of the mooring design variable in the design procedure to minimise time and
35 57 effort by eliminating the rigorous trial and error approach, and by considering the mooring design
36 58 variables as optimisation variables.
37
38

39
40 59 To actualise this, several studies on the optimization of mooring line design parameters utilising
41 60 different optimization techniques have been conducted to address the optimization of the mooring
42 61 system. Maffra et al., [6] were the first to apply the Genetic Algorithm (GA) in mooring system
43 62 optimization, with the primary objective of minimising offset of a spread moored vessel through
44 63 the optimisation of the mooring line radius. A mooring pattern optimization of a vessel with a
45 64 multi-point mooring system was presented in [7] using the Steady-State Genetic Algorithm
46 65 (SSGA). Also, Mehdi and Rezvani [5] proposed another mooring optimisation procedure using a
47 66 different variant of GA called Constrained Genetic Algorithm (CGA), the primary objective was
48 67 to minimise platform offset in surge and sway directions by optimizing azimuth angle, mooring
49 68 radius and the line length. Unlike the preceding procedure, Liang et al [8] proposed a multi-
50 69 objective procedure utilising the Non-dominated Sorting Genetic Algorithm II (NSGA-II) to
51 70 optimise several mooring design variables in addition to the platform offset and having the
52 71 capability of providing multiple optimal mooring design.
53
54
55
56

57 72 The application of the Particle Swarm Optimization (PSO) technique was first used for mooring
58 73 line optimization by [9] with the objective function of minimising platform offset by considering
59 74 mooring radius and line azimuth angles as the optimisation parameters. An appreciable reduction
60
61

1
2
3
4 75 in platform offset was recorded in the range of 30% and 60% for the two models considered in the
5 76 work. Furthermore, Monteiro et al [10] assess the implementation of an improved PSO (POSI)
6 77 technique using line mooring radius, azimuth angle, pretension and line material as optimisation
7 78 variables. The PSOI, when compared with the standard PSO is reported to have an improved
8 79 convergence rate which is achieved by the application of a velocity update component. The
9 80 integrated mooring-riser design methodology was also adopted where the riser safe operation
10 81 (SAFOP) zone diagrams in combination with the mooring line offset diagrams were used to
11 82 account for the integrity of the risers. The application of a variant of the PSO algorithm associated
12 83 with an ϵ -constrained was also applied [11] for the optimisation of deep-water semisubmersible
13 84 platform using mooring radius, line length and pretension as optimisation variables. However, this
14 85 procedure is an improvement of the one presented in [10] with the introduction of a constrained
15 86 function to efficiently handle constraints and enhance the evaluation of candidate solutions by
16 87 adopting full non-linear time-domain FE simulations with a coupled model. A more complex
17 88 approach considering asymmetric mooring configurations was considered in [12] taking each of
18 89 the line azimuth angles and mooring radius as optimization variables. The study compares the
19 90 performance of differential evolution and PSO based on their convergence capability. This was
20 91 implemented as a spread mooring system of a deep-water semi-submersible platform. In recent
21 92 times, Montasir *et al.*, [3] proposed a standalone mooring optimisation tool based on quasi-static
22 93 analysis. The line azimuth angle was used as an optimization variable and successfully
23 94 implemented using PSO. The proposed tool has optimised offset of a truss spar offset by up to
24 95 72% when compared with the original model. However, most of the procedures presented utilised
25 96 either static or dynamic in the analysis of mooring lines.

26
27
28
29
30
31
32
33
34 97 Over the years, the interaction between mooring lines and risers has been recognised as an
35 98 important design consideration, particularly in deep-water operations [11, 13-16]. As a result, an
36 99 integrated design methodology has been demonstrated as a better alternative, where the risers,
37 100 moorings, and floaters are all analysed simultaneously to create a SAFOP and offset diagrams for
38 101 the riser and moorings respectively. The inclusion of risers in the analysis of floating platforms
39 102 has been reported as having a significant influence on their natural periods, damping, as well as
40 103 slow drift responses [17]. In another study [18], the inclusion of risers in the analysis was found to
41 104 have considerable contributions to surge/sway coupling, and as a result the low-frequency motion
42 105 response. For this reason, the integrated riser-mooring design methodology was regarded as
43 106 potentially beneficial in deep water platform operations, particularly in terms of the overall system
44 107 safety, response, and cost[14].
45 108 By incorporating all the components in a single model throughout the study, the technique enable
46 109 s for efficient incorporation of the interaction between the riser, mooring, and platform [12, 18].
47 110 Furthermore, previous studies have demonstrated the inclination of the oil and gas industries
48 111 toward full integration of the mooring and riser design procedure[4, 19].

49
50
51
52
53
54 112 Thus, this paper presents an optimisation procedure of mooring line design parameters using the
55 113 Mooring Optimisation Tool for FPSO (MooOpT4FPSO). The tool is an in-house optimization tool,
56 114 which is an integration of the Regrouping Particle Swarm Optimization (RegPSO) algorithm and
57 115 OrcaFlex. The tool has the capability of optimising mooring line parameters of turret FPSO
58 116 supported with 12 or 9 mooring lines. In addition, the tool is configured to take into consideration

of the mooring line parameters, it is not limited by the position of the turret or the type of mooring line system (catenary or taut), thus can be utilised for both internal and external turret. Utilizing the tool, mooring line design parameters; mooring line diameter, line length (middle segment), mooring radius, and azimuth angles of a turret FPSO were simultaneously optimised. The integrated mooring-riser methodology was incorporated to consider the interaction of the riser in the procedure. The paper considered twelve mooring lines azimuth angles, line diameter, mooring radius, and line length as optimization variables. The superimposition of the riser safe operation (SAFOP) zone and the offset diagram reveals the optimised mooring parameters as sufficient in maintaining platform offset within the SAFOP Apart from successfully having the capability of optimising the platform offset, the tool has the flexibility of utilising the robust capability of the OrcaFlex software utilising both static and dynamic analysis.

1.1 Selection of Optimization variables

The mooring system considered in this study is an internal turret consisting of taut and **catenary** mooring lines. This version of MooOpT4FPSO has the capability of optimising mooring line parameters of turret FPSO with 12 and 9 lines, i.e., 4x3 and 3x3 mooring configuration respectively as illustrated in Figures 1(a, b). Each of the lines comprises a chain-polyester -chain segment distributed equally and at the same pretension characteristic value of 1420kN. The mid-section of each of the mooring lines is of the same length and diameter. Thus, the mooring line design variable of each line identified to influence the performance of the mooring system was adopted as the optimization variable. For each of the mooring configurations, the azimuth angles of the central lines of each group, i.e., lines #1,2,3,4 for 4x3 or lines #1,2,3 for 3x3, are considered optimization parameters. Thus, MooOpT4FPSO considers a total of 7 or 6 mooring line parameters as optimisation parameters, i.e., 4 or 3 azimuth angles, in addition to mooring radius, mooring line length (of mid-segment) and line diameter. The case is automatically selected depending on the number of mooring lines defined by the user.

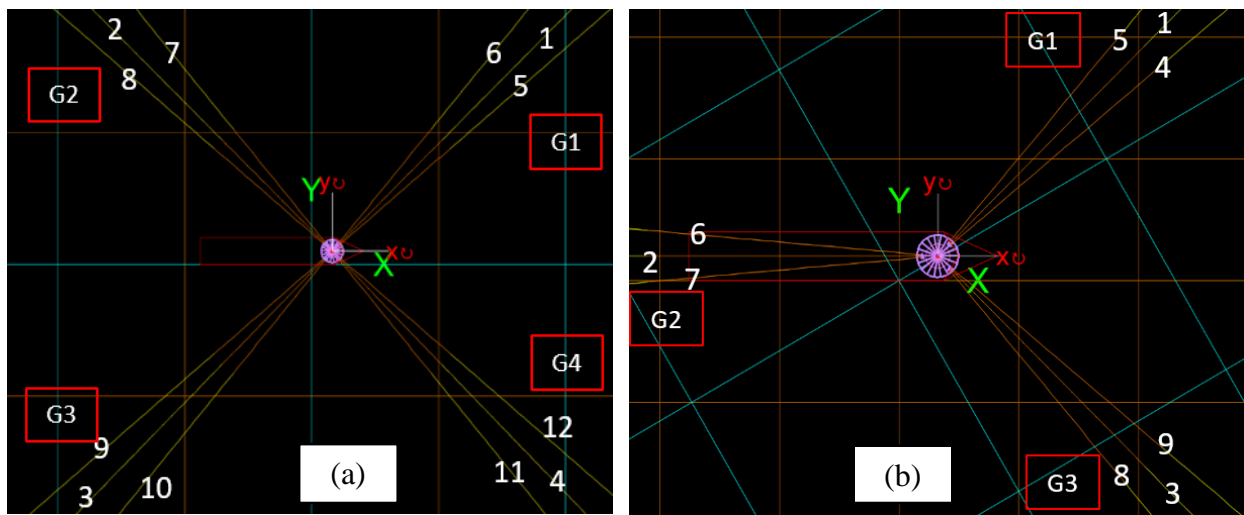


Figure 1: Layout of turret mooring configuration: (a) 4 x 3 configuration (b) 3 x 3 configuration

1.2 Objective function

The problem presented here is a typical constrained optimisation problem, expressed mathematically in Equation 1. The aim is to minimize the objective function $f(x)$ which in this case is the FPSO surge offset. Thus, the primary objective of the optimization procedure is to optimise line parameters that will minimise surge offset of turret FPSO, which has been identified as the most sensitive response.

$$\text{minimize } f(\text{offset}) \quad (1)$$

$$\text{subject to } g_i(\text{offset}) \leq \text{threshold of success}, \quad i, \dots, m$$

Where the *threshold of success* is the maximum allowable platform offset defined for the problem, while $g_i(\text{offset})$, is the global best platform offset for each iteration.

The integrated riser-mooring design methodology elaborated in [1, 14] and adopted in [2] has been incorporated herein. Adopting this approach as a component of the optimization procedure is considered more realistic in terms of ensuring the interaction of risers is taken into consideration. This methodology ensures the platform excursion/offset is maintained within the riser safe operation zone (SAFOP).

Thus, the objective of the integrated riser-mooring design methodology is expressed in Equation (2)

$$f = \frac{\sum_{i=1}^{ndir} SAFOP(i) - \text{platform offset}(i)}{ndir} \quad (2)$$

where, i is the number of directions considered ($i = 1, ndir$), which should be at least 8, $SAFOP(i)$ is the riser safe operation zone in each direction, i recorded in meters, while $\text{platform offset}(i)$ is the platform excursion obtained using the mooring system, and in the same directions.

1.3 Constraints

The maximum allowable mooring tensions are based on the guidance provided in section 7.2 of the API-RP-2SK[20] specifying 60% and 80% of the minimum breaking load (MBL) when considering dynamic analysis in intact and damage conditions respectively. Thus, the tension constraints are expressed in Equations (3).

$$CTsn_{max} = \begin{cases} \frac{Tsn_{max}}{MBL} - 0.6, & \text{if } \frac{Tsn_{max}}{MBL} \geq 0.6 \\ 0, & \text{Otherwise} \end{cases} \quad (3)$$

Where, Tsn_{max} is the maximum mooring tension in all lines of a given candidate solution.

2 The Optimisation Tool

2.1 Mooring Optimization Tool for FPSO

The in-house optimization tool named Mooring Optimization Tool for FPSO (MooOpT4FPSO) is a numerical optimization tool developed to optimize mooring line design parameters of turret moored FPSO. The tool is an integration of a Regrouping Particle Swarm Optimisation (RegPSO)

1
2
3
4
5
6
7
8
9
10
11
12
13
14
15
16
17
18
19
20
21
22
23
24
25
26
27
28
29
30
31
32
33
34
35
36
37
38
39
40
41
42
43
44
45
46
47
48
49
50
51
52
53
54
55
56
57
58
59
60
61
62
63
64
65

algorithm with OrcaFlex. This version of MooOpT4FPSO has the capability of simultaneously optimizing azimuth angles, mooring line lengths, line diameter and mooring radius of an FPSO turret mooring system consisting of 9 and 12 mooring lines.

MooOpT4FPSO communicate with OrcaFlex in the MATLAB environment through the dynamic link library. Implementation of the optimization procedure includes a complete definition of the FPSO model including the mooring system and environmental loading in OrcaFlex. The OrcaFlex data file is then utilised by the RegPSO algorithm in the MATLAB environment to initialise and assign the mooring line parameters to each line in the OrcaFlex model from a user-defined range. The initialisation of the population of candidate solutions is randomly generated and iteratively updated in the process. For each iteration, dynamic analysis is performed, and a set of mooring line parameters is saved. In each case, individual candidate solutions are evaluated to assess their fitness by the objective function which in turn guides the search process to an optimum solution[1]. This procedure is repeated based on the defined number of particles and iterations until an optimised solution is obtained. An optimised solution here refers to mooring line parameters that yield the minimum platform offset. Figure 2 illustrates the data flow diagram of the optimization tool.

The developed optimisation tool has an interactive Graphical User Interphase which as illustrated in Figure 3 has 5 major components, namely: (1) the OrcaFlex Path; where the user specifies the path of OrcaFlex on the computer (2) User-defined input; this is where the user defines the optimization and line parameters. (3) The Run, Plot, and Log tabs. (4) Outcomes of optimization; here the optimized mooring line parameters are displayed, and (5) the plot area; the plan of optimized lines with their azimuth angles are displayed.

Firstly, implementation of the optimization procedure requires the user to define the OrcaFlex path on the computer. Secondly, the mooring design parameters and optimization settings are defined. Using the run tab, the optimization process is started. Upon completion of the optimization process, the plot is generated using the plot tab. To view the detail of optimization settings or error reports the Log tab is used.

1
2
3
4
5
6
7
8
9
10
11
12
13
14
15
16
17
18
19
20
21
22
23
24
25
26
27
28
29
30
31
32
33
34
35
36
37
38
39
40
41
42
43
44
45
46
47
48
49
50
51
52
53
54
55
56
57
58
59
60
61
62
63
64
65

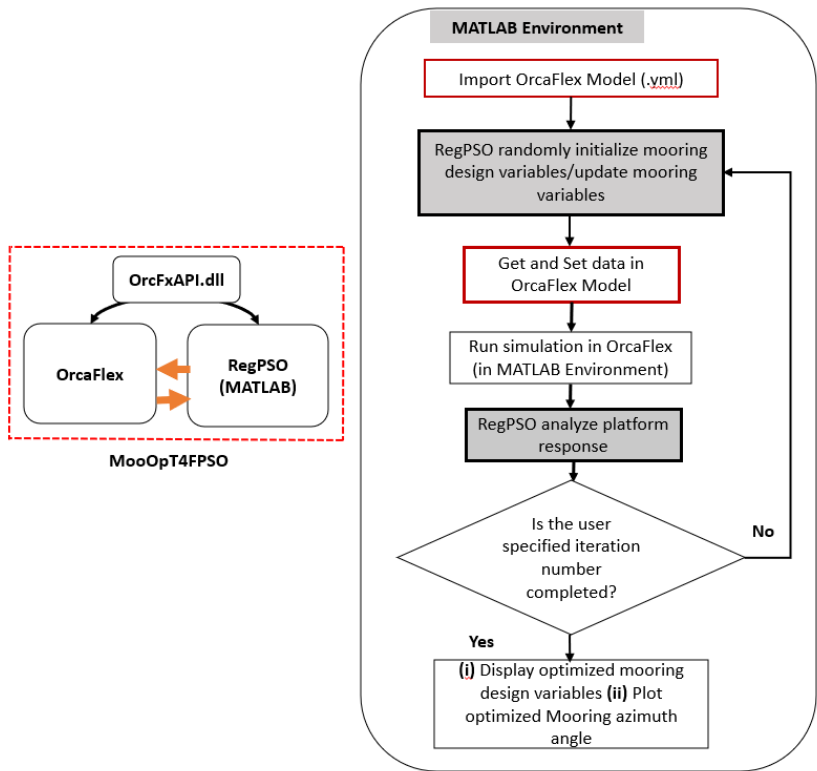


Figure 2: Data flow working diagram of the optimisation tool (MooOpt4FPSO)

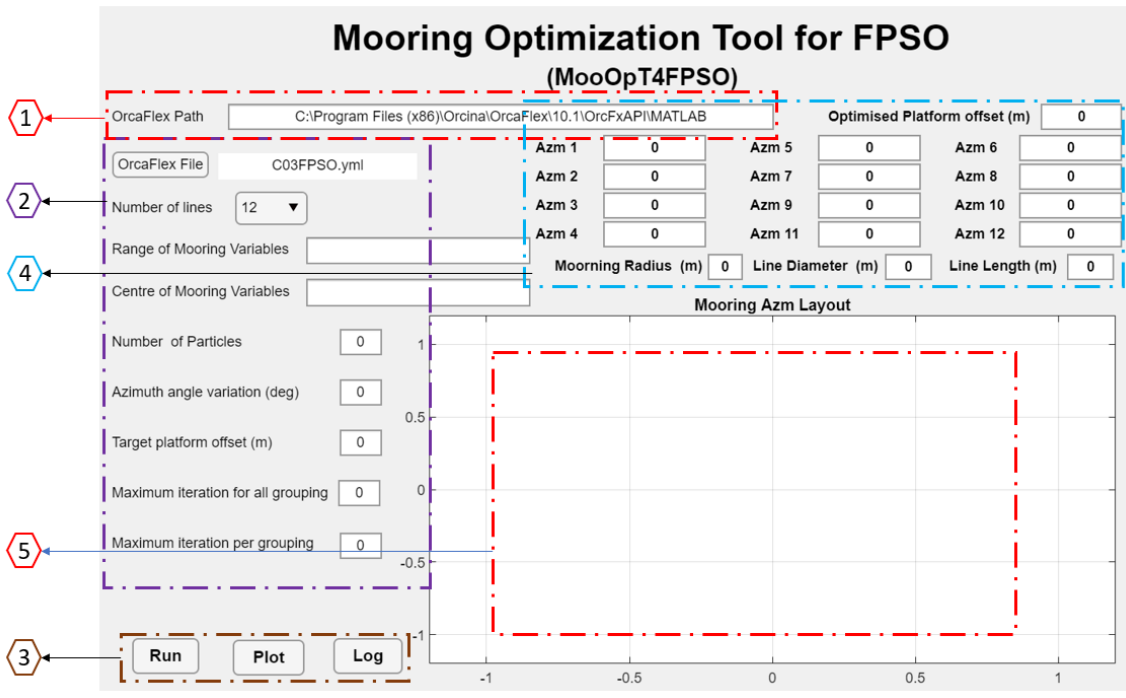


Figure 3: Graphical User Interface of MooOpt4FPSO illustrating the major component

1
2
3
4 218
5
6 219
7
8 220
9 221
10 222
11 223
12 224
13
14 225
15 226
16 227
17 228
18 229
19
20 230
21 231
22 232
23 233
24
25 234
26 235
27 236
28 237
29
30 238
31 239
32 240
33 241
34
35 242
36 243
37 244
38 245
39 246
40
41 247
42 248
43
44
45
46
47
48
49
50
51
52
53
54
55
56
57
58
59
60
61
62
63
64
65

2.2 Regrouping Particle Swarm Optimisation

The Regrouping Particle Swarm Optimization (RegPSO) technique is a variant of the PSO developed to address the problem of premature convergence identified as a shortcoming of the standard PSO algorithm [21]. The algorithm has the computational capability to identify when premature convergence (viz, stagnation) occurs and regroup the particle into a new search space large enough to allow for an efficient search to enable them to escape stagnation and allow the entire swarm to continue making progress rather than restarting as proposed in other studies [22]. It is important to note that the standard PSO is effective before being prematurely converged. Thus, the RegPSO algorithm still utilizes the original position and velocity update equations. Hence the main improvement is to liberate the swarm from premature convergence via an automatic regrouping mechanism. Figure 4 illustrates the flow chart of the RegPSO algorithm.

All particles are randomly picked from all the problem dimensions toward the global best by using the update Equations in 4 and 5.

$$\vec{x}_i(k + 1) = \vec{x}_i(k) + \vec{v}_i(k + 1) \tag{4}$$

$$\vec{v}_i(k + 1) = w\vec{x}_i(k) + c_1\vec{r}_1(k) \circ (\vec{p}_i(k) - \vec{x}_i(k)) + c_2\vec{r}_2(k) \circ (\vec{g}_i(k) - \vec{x}_i(k)) \tag{5}$$

Where k is the current iteration, \vec{v}_i is the velocity vector, \vec{x}_i is the position vector of particle i while w is the static inertia weight. c_1 and c_2 stand for cognitive and social acceleration coefficients respectively, \vec{p}_i is the personal best of particle i and \vec{g}_i the global best of the swarm. The \vec{r}_1 and \vec{r}_2 are n -dimensional column vectors consisting of pseudo-random numbers selected from a uniform distribution.

1
2
3
4
5
6
7
8
9
10
11
12
13
14
15
16
17
18
19
20
21
22
23
24
25
26
27
28
29
30
31
32
33
34
35
36
37
38
39
40
41
42
43
44
45
46
47
48
49
50
51
52
53
54
55
56
57
58
59
60
61
62
63
64
65

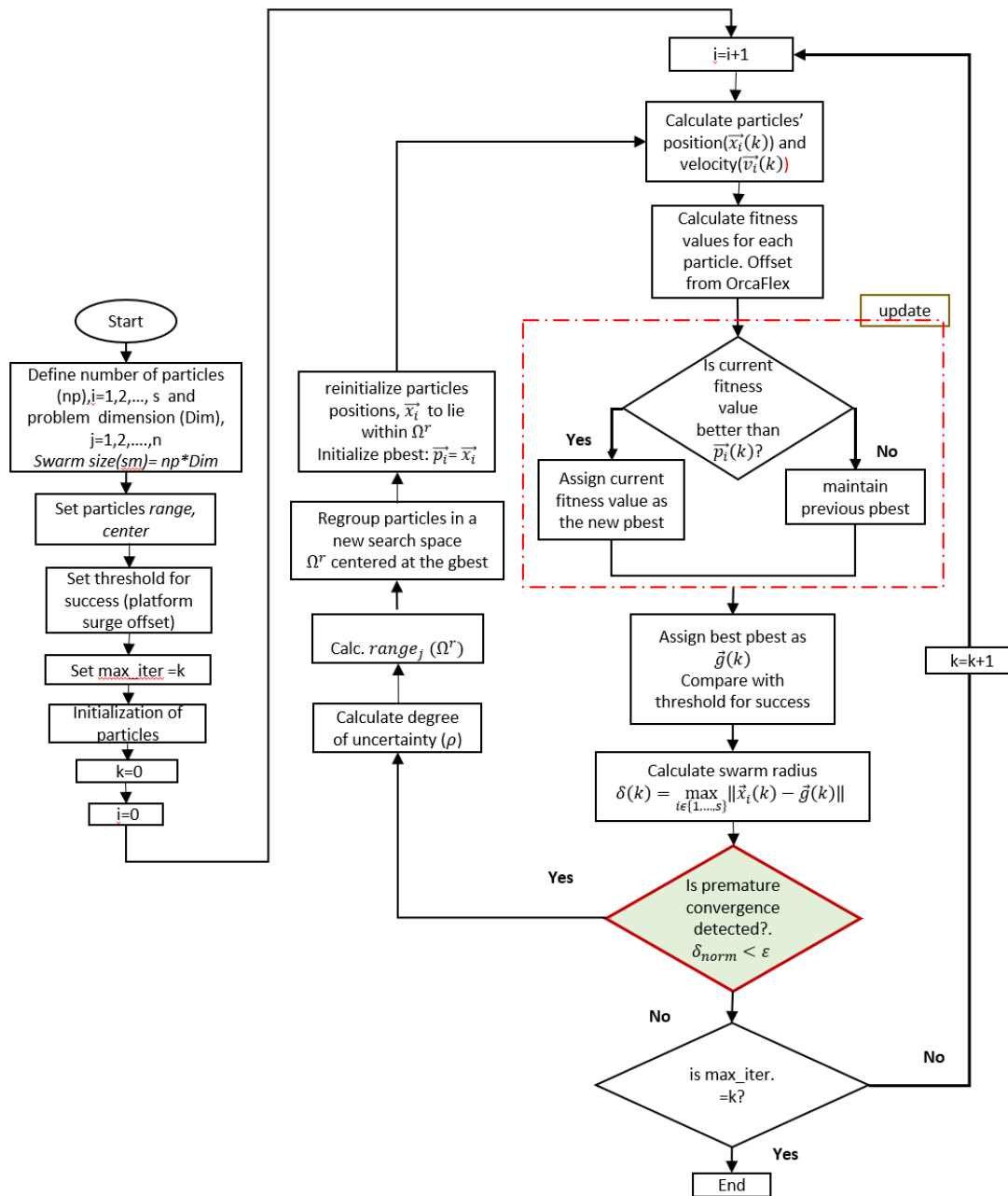


Figure 4: Flow chart of RegPSO algorithm

2.2.1 Detection of Premature Convergence

Depending on the number of particles defined in the process, some particles may fail to find a better solution (i.e., a new global best) over a long simulation time, in which case, the particle will tend to continue to move closer to the unchanged global best until all other particles eventually prematurely converged (occupy the same location in space), thereby approximating a local solution rather than a global one. Consequently, progress toward the global best will cease and the process will instead continue to refine the local minimizer with no room for further improvement.

For this reason, the RegPSO determine the distance between the particles as a measure of how close they are to each other to monitor when they eventually converged to the same region or stagnate. This occurrence (premature convergence) is detected from the measurement of maximum swarm radius between particles using Equation 6, initially introduced by Van den Bargh [23]. For each iteration, the swarm radius $\delta(k)$ is calculated in the n- dimensional space of any particle from the global best.

$$\delta(k) = \max_{i \in \{1, \dots, s\}} \|\vec{x}_i(k) - \vec{g}(k)\| \quad (6)$$

If Ω is considered as the search space and the range of particle dimensions represented by the vector, $\overline{range}(\Omega)$. Then, the diameter of the search space is taken as $dia(\Omega) = \|\overline{range} \Omega\|$. The particles are considered too close to each other when the normalized swarm radius (δ_{norm}) is less than the stagnation threshold (ε) as depicted in Equation (7).

$$\delta_{norm} = \frac{\delta(k)}{dia(\Omega)} < \varepsilon, \text{ where } \varepsilon = 1.1 \times 10^{-4} \quad (7)$$

2.2.2 Regrouping of Swarm

Once the condition in Equation (7) is met (i.e., premature convergence detected), the swarm is automatically regrouped into a new search space centred on the global best, using the regrouping factor shown in Equation (8).

$$\rho = \frac{6}{5\varepsilon} \quad (8)$$

The range of each problem dimension defining the new search space, Ω^r are determined by either the magnitude of the regrouping factor, ρ , or the degree of uncertainty inferred on each dimension from the maximum deviation from the global best.

It is important to state here that the degree of uncertainty on each of the dimensions overall particles is computed using Equation (6) while Equation (9) is used to compute the maximum deviation of any one particle.

$$range_j(\Omega^r) = \min \left(range_j(\Omega^r), \rho \max_{i \in \{1, \dots, s\}} |x_{i,j}(k) - g_j(k)| \right) \quad (9)$$

In each case, each particle is randomly regrouped about the global best within the new search space (Ω^r) according to equation (7), this process makes the randomized particle remain within the Ω^r with respect to the defined lower and upper bounds defined in Equations (12) and (13).

$$\vec{x}_i(k+1) = \vec{g}_i(k) + \vec{r}_i \cdot \overline{range}(\Omega^r) - \frac{1}{2} \cdot \overline{range}(\Omega^r) \quad (10)$$

Where, \vec{r}_i is a vector of the problem dimension

$$[r_1, r_2, \dots, r_n] \quad (11)$$

1
2
3
4
5
6
7
8
9
10
11
12
13
14
15
16
17
18
19
20
21
22
23
24
25
26
27
28
29
30
31
32
33
34
35
36
37
38
39
40
41
42
43
44
45
46
47
48
49
50
51
52
53
54
55
56
57
58
59
60
61
62
63
64
65

$$297 \quad x_j^{L,r} = g_j - \frac{1}{2} range_j(\Omega^r) \quad (12)$$

$$298 \quad x_j^{U,r} = g_j + \frac{1}{2} range_j(\Omega^r) \quad (13)$$

300 L and U in Equations 9 and 10 represent lower and upper limits respectively.

301 Once the regrouping of the particle is implemented as highlighted in the preceding section, the
302 standard PSO continues as usual. This procedure is repeated iteratively.

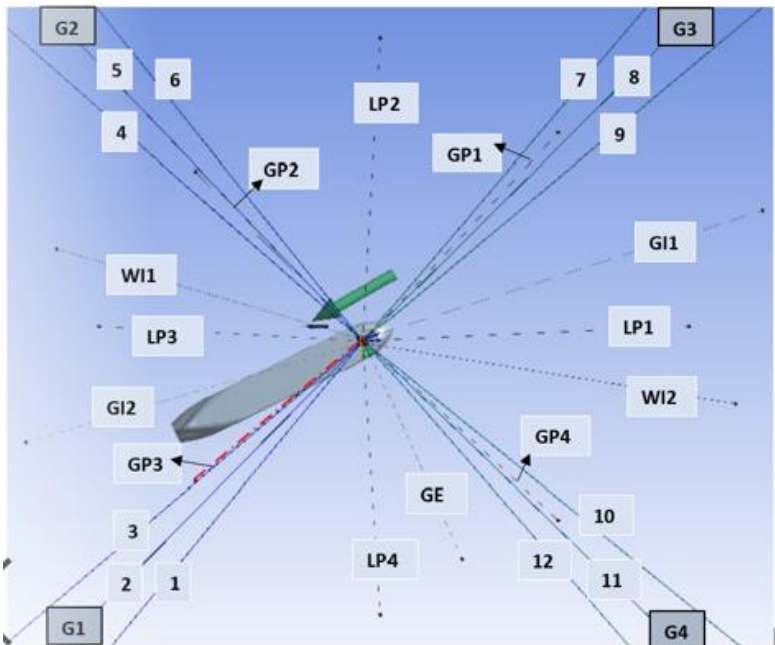
304 2.3 OrcaFlex

305 OrcaFlex is a 3D non-linear finite element software used for the design and analysis of offshore
306 oil and gas structures and Marine systems such as mooring systems, risers, and marine renewables.
307 It has the capabilities of performing Static and dynamic analysis, fatigue analysis and modal
308 analysis, etc. It also has the capability of implementing both quasi-dynamic and fully coupled
309 analysis.

310 3 Description of Model

311 3.1 The FPSO Model

312 In implementing the optimisation procedure, a validated turret moored FPSO model was used as
313 in[24]. The model consists of 12 multi-component mooring lines configured into 4 groups, each
314 group consisting of 3 lines, in addition to 13 steel catenary risers as shown in Figure 5. The FPSO,
315 mooring line and riser system design parameters are depicted in Tables 1, 2 and 3.



316
317 Figure 5: Layout of Mooring-riser systems of turret FPSO

Table 1: FPSO main design parameter [24]

Parameter	Symbol	Unit	Quantities
Vessel size		kDWT	200
Length between perpendicular	L_{pp}	m	310
Breadth	B	m	47.17
Height	H	m	28.04
Draft (80% loaded)	T	M	15.121
Displacement	V	MT	186051
Block coefficient	C_b		0.85
Surge centre of gravity from turret	CGx	m	-109.67
Heave centre of gravity from mwl	CGy	m	-1.8
Frontal wind area	A_F	m ²	4209.6
Transverse wind area	A_T	m ²	16018.6
Roll radius of gyration at CG of turret	R_{xx}	m	14.036
Pitch radius of gyration at CG of turret	R_{yy}	m	77.47
Yaw radius of gyration at CG of turret	R_{zz}	m	79.3
Turret in center line behind F_{pp}	Xtur	m	38.75
Turret diameter	Dtur	m	15.85
Turret elevation below tanker base		m	1.52

Table 2: Mooring line Details [24]

Legend	Top Segment	Middle Segment	Lower Segment
Type	Chain	Polyester	Chain
Diameter(mm)	95.3	160	95.3
Length (m)	91.4	2438	91.4
Wet weight (kg/m)	164.63	4.5	164.63
Effective Modulus (kN)	820900	168120	820900
Breaking Load (kN)	7553	7429	7553
Normal drag coefficient, C_{DN}	2.45	1.2	2.45
Normal added inertia coefficient, C_{IN}	2.0	1.15	2.0

Table 3:Particulars of Steel Catenary Risers

	LP	GP	WI	GI	GE
Top tension (kN)	1112.5	609.7	2020.0	1352.8	453.9
Outer diameter(mm)	444.5	386.1	530.9	287.0	342.9
EA (kN)	18.3 x10 ⁶	10.3 x10 ⁶	18.6 x10 ⁶	31.4 x10 ⁶	8.6 x10 ⁶
Wet Weight (N/m)	1037	526	1898	1168	423

3.2 Environmental Data and Prediction of Wind and Current Forces

The study was conducted using a water depth of 1829m considering 100-year hurricane conditions of the Gulf of Mexico. The JONSWAP wave spectrum having a significant wave height of 12.19m and a peak period of 14 seconds acting at 180 degrees was used as illustrated in Figure 6. The wind loading was generated using the Norwegian Petroleum Directorate (NPD) spectrum at 150degrees with a mean velocity of 41.12m/sec acting at 10m height. In addition, a current profile with a varying velocity of 0.941m/s to 0.0941m/sec from mean sea level to the sea bed is used[24].

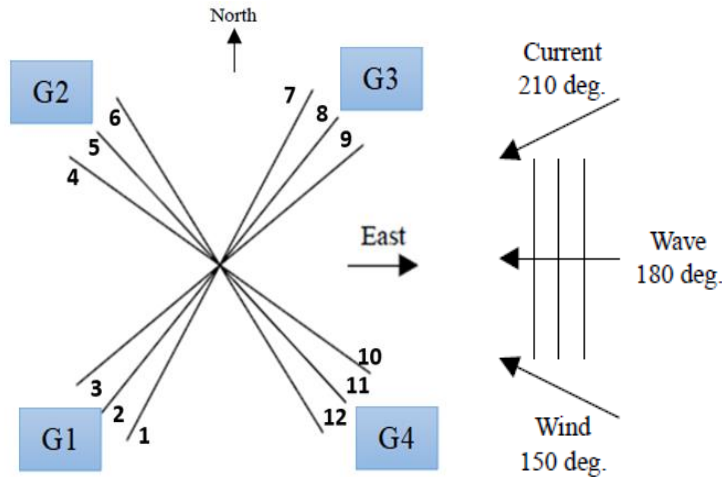


Figure 6: Illustration of the wave, wind, and current directions

3.3 Functionality of RegPSO

To determine the functionality of the RegPSO component of the tool, the RegPSO algorithm is validated using seven mathematical benchmark functions, including Ackley, the Griewangk, Quadric, Quartic Noise, Rastrigin, Rosenbrock, and weighted sphere as detailed in Table 3. These benchmarks were tested based on a varying number of particles and iterations. In each case, the problem dimension was maintained as 10, with a maximum of 30 particles at 250 iterations. The percentage of range to which each dimension is to be clamped (i.e., velocity clamping) is

350 maintained at 15% as recommended by Liu et al.,[25] because it performs better than the traditional
 351 50%.

352 Table 3: Benchmark Functions

Benchmarks	Function	Initial range of x_j
Ackley	$f(\vec{x}) = 20 + e - 20e^{-0.2\sqrt{\frac{\sum_{j=1}^n x_j^2}{n}}} - e^{\frac{\sum_{j=1}^n \cos(2x_j\pi)}{n}}$	$-32 \leq x_j \leq 32$
Griewangk	$f(\vec{x}) = 1 + \sum_{j=1}^n \frac{x_j^2}{4000} \prod_{j=1}^n \cos\left(\frac{x_j}{\sqrt{j}}\right)$	$-600 \leq x_j \leq 600$
Quadric	$f(\vec{x}) = \sum_{j=1}^n \left(\sum_{j=1}^n j \cdot x_j \right)^2$	$-100 \leq x_j \leq 100$
Quartic Noise	$f(\vec{x}) = \text{random}(0,1) + \sum_{j=1}^n j \cdot x_j^4$	$-1.28 \leq x_j \leq 1.28$
Rastrigin	$f(\vec{x}) = 10n + \sum_{j=1}^n (x_j^2 - 10\cos(2x_j\pi))$	$-5.12 \leq x_j \leq 5.12$
Rosenbrock	$f(\vec{x}) = \sum_{j=1}^{n-1} (100(x_{j+1} + x_j^2)^2 + (x_j)^2)$	$-30 \leq x_j \leq 30$
Weighted Sphere	$f(\vec{x}) = \sum_{j=1}^n j \cdot x_j^2$	$-5.12 \leq x_j \leq 5.12$

353 These functions are selected to test the computational capability of the RegPSO algorithm to
 354 optimize both uni-modal and multimodal functions. For example, Ackley, Rastrigin, and
 355 Rosenbrock's functions are multi-modal while weighted sphere and the Griewangk's functions are
 356 unimodal. In each case, the existence of local minima tends to increase with increasing problem
 357 dimensionality. In this case, considering the mooring line design variables are less than 10, so we
 358 maintain a maximum dimension of 10 to test the capability by varying the number of particles and
 359 iterations. For each function, two trial was conducted to allow for average comparison.

3.4 Implementation of the Optimisation Procedure

363 The tool utilises an updated OrcaFlex data file linked with the RegPSO code to automatically
 364 search and update mooring design variables taking advantage of the robust functionality of the
 365 software. The functionality of the tool is influenced by many parameters, including the number of
 366 particles, dimension of the problem, number of iterations and other parameters as listed in Table
 367 4. The number of particles particularly dictates the size of the swarm (i.e., swarm = no of particle

* dimension). However, although the larger the number of particles the greater the chances of finding a global minimum, this can also result in parallel random search and in that case increasing the computational time. A varying number of particles ranging from 10 - 50 have been reported as appropriate for different variants of PSO [26]. On the other hand, the number of iterations together with the specified success threshold dictate the stopping criteria.

For each mooring variable, a range and central (median) value is defined to guide the search of the protocol to the global best.

Table 4: RegPSO parameter setting

Parameter	Value
Number of particles	Up to 10
Dimension of problem	6 and 7
Stagnation threshold	$1.1 \cdot 10^{-4}$
Regrouping factor	$1.2 / \text{Stagnation threshold}$
Inertia weight	[0.9,0.4]
Max velocity clamping %	0.15
No. of iterations per group	varied
Max iteration overall grouping	varied

3.5 Integrated Design Methodology

Previously, some of the few available mooring optimisation procedures considered only the mooring lines for the prediction of optimal platform offset without due consideration to the integrity of the risers [3, 4]. In this study, we incorporated the integrated design methodology which is implemented based on the flow chart illustrated in Figure 7. The procedure of producing SAFOP and offset diagrams.

The SAFOP is a polar diagram defining the horizontal displacement within which the top and the bottom connection point of the risers must remain to ensure none of the risers exceeds any of its design criteria in any of the wave directions considered. Here, we considered the 8 wave directions in producing the diagrams.

The offset diagrams on the hand are also polar diagrams that define the expected maximum horizontal excursions of the floater.

The superposition of the two diagrams gives a visual verification/assessment of the design criteria for the riser and mooring lines.

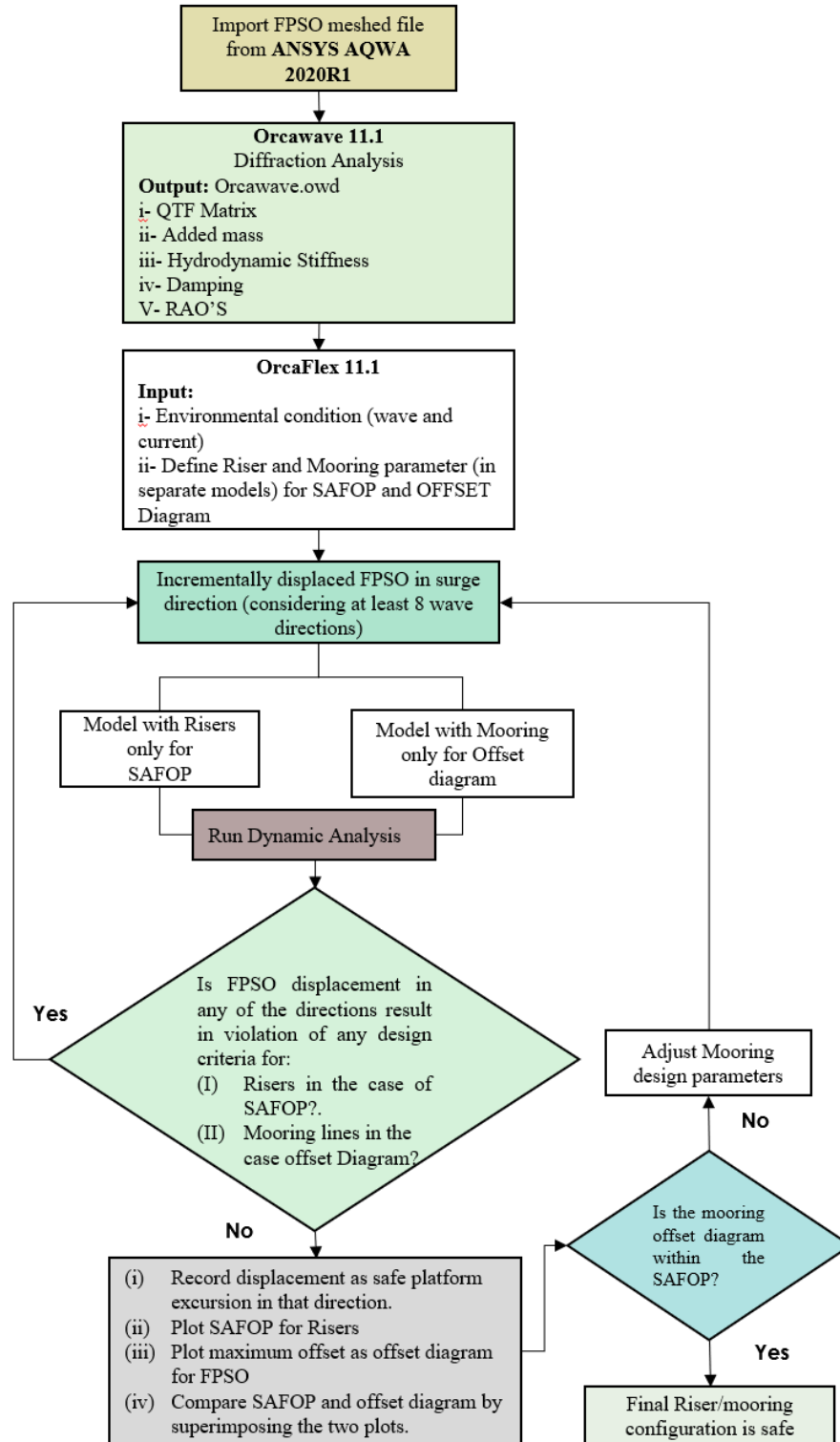


Figure 7: Flow chart for implementation of Safe Operation Zone (SAFOP) and offset Diagram for the Mooring system

4 Results and Discussions

4.1 Validation of FPSO model for hydrodynamic data

The validation results (AQWA) consisting of static offset, free decay, and hydrodynamic response results in six degrees of freedom (6DOF) degrees well with the published results [3] as shown in Figure 6, Tables 5 and 6 respectively. Figure 8 compares the mooring restoring forces from both models, which tend to linearly increase with increasing platform excursion. However, a slight variation of 3% between the WINPOST and AQWA model is observed at about 80m to 90m excursions.

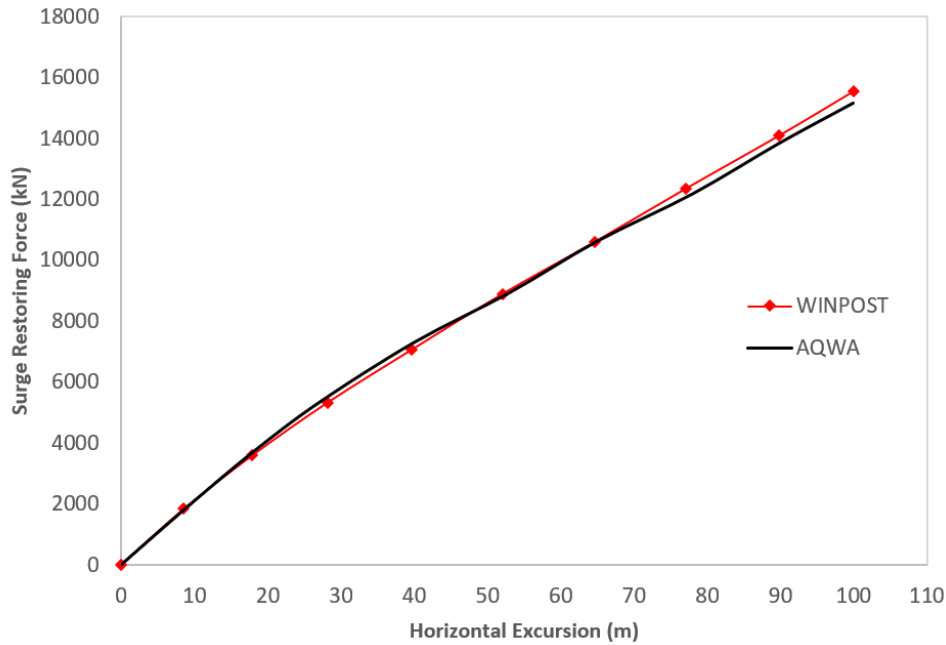


Figure 8: Comparison of Restoring Behaviour of the WINPOST and AQWA model

From Table 5, the natural periods of the AQWA model for all the degrees of freedom considered are within the range of both published experimental and simulation results. The same trend is observed in the case of the damping ratios, with the AQWA model having damping ratios closer to the published experimental results. Overall, the results compare well with the published restoring force, natural periods, and damping ratios.

Table 5: Comparisons of Validation free decay results

	Periods(sec)			Damping (%)		
	AQWA	WINPOST	OTRC	AQWA	WINPOST	OTRC
Surge	205.2	204.7	206.8	3.7	4.4	3.0
Heave	10.8	10.8	10.7	4.5	11.8	6.7
Roll	12.7	12.7	12.7	3.2	0.7	3.4
Pitch	10.7	10.8	10.5	7.5	10.5	8.0

Table 6 statistically compares the responses of the AQWA model in 6DOF with the published results. This reveals close agreement with the published results, thereby proving the accuracy adopted in the validation process.

Table 6: Comparison of validation results in 6DOF

	Source	Surge(m)	Sway(m)	Heave(m)	Roll (deg)	Pitch (deg)	Yaw (deg)
Max	AQWA	4.44	11.2	8.33	8.2	3.37	-15.21
	WINPOST	2.29	13.1	10.9	3.5	4.45	-3.4
	OTRC	6.30	10.9	9.11	9.57	4.2	-8.69
Min	AQWA	-60.22	-20.04	-10.45	-7.26	-4.37	-29.72
	WINPOST	-61.30	-21.4	-11.3	-3.6	-4.99	-24.6
	OTRC	-54.10	-13.6	-9.52	-8.77	-4.07	-23.3
Mean	AQWA	-20.77	-0.48	0.11	0.06	0.17	-18.37
	WINPOST	-22.90	-0.09	0.14	-0.1	0.01	-16
	OTRC	-21.10	-0.64	-0.06	-0.08	0.03	-16.8
SD	AQWA	7.97	4.55	2.92	1.45	1.19	5.03
	WINPOST	9.72	4.57	3.08	0.9	1.31	3.8
	OTRC	8.78	4.05	2.81	2.18	1.26	2.46

4.2 The Functionality of the RegPSO Algorithm

Table 7 shows the statistical performance of RegPSO code in optimising various mathematical benchmark functions with a different number of particles. It can be observed that with an increasing number of particles the global minima also decrease. This is due to the consequent increase in swarm size which increases the number of possible solutions. Thus, this indicates the capability of the RegPSO in finding the optimum solution for the selected mathematical benchmark functions.

For the mean of the two trials conducted for each benchmark, it can be observed that the code has successfully minimised Ackley function by 99%, the Griewangk function by 90%, Quadric by 99.9% and Quartic Noisy by 96.1%. The code also minimises Rastrigin by 82%, Rosenbrock by 98% and weighted sphere by 100%. The Rastrigin benchmark function result is particularly impressive because the benchmark generally returns high function values due to the stagnation of the swarm.

Table 8 shows the statistical comparison of RegPSO performance across seven benchmark functions with an increasing number of iterations. A similar trend was observed in Table 7. The code was able to minimise the Ackley function by 97%, the Griewangk function by 72%, the Quadric function by 99% and Quartic Noisy by 80%. It has also minimised the Rastrigin function by 56%, Rosenbrock function by 58% and weighted sphere by 99%.

Table 7: Functionality of RegPSO across Mathematical benchmarks with different numbers of particles

Benchmark functions	Dimension	No. particle		Number of particles		
				2	10	30
Ackley	10	30	Mean	6.6583	0.16809	0.07034
			min	4.519	0.11141	0.05609
			max	8.7979	0.22476	0.08459
			std	3.0254	0.08015	0.02015
Griewangk	10	30	Mean	1.9885	0.46766	0.19584
			min	1.5313	0.36529	0.12548
			max	2.4458	0.57004	0.2662
			std	0.64665	0.14478	0.0995
Quadric	10	30	Mean	1397.62	4.3421	0.87772
			min	616.936	1.9549	0.23309
			max	2178.3	6.7294	1.5223
			std	1104.05	3.3761	0.91165
Quartic Noisy	10	30	Mean	0.14832	0.01337	0.00578
			min	0.13059	0.00732	0.0047
			max	0.16605	0.01942	0.00685
			std	0.02507	0.00856	0.00152
Rastrigin	10	30	Mean	41.6264	14.8883	7.5733
			min	38.5929	4.8645	7.1779
			max	44.6599	24.9121	7.9686
			std	4.29	14.1758	0.55905
Rosenbrock	10	30	Mean	4344.47	367.807	85.7507
			min	3761.15	207.586	72.4246
			max	4927.79	528.027	99.0768
			std	824.941	226.586	18.8459
weighted Sphere	10	30	mean	2.8269	0.00045	0.00028
			min	1.1083	0.00034	0.00028
			max	4.5455	0.00055	0.00029
			std	2.4305	0.00015	1.31E-05

446
447

Table 8: Functionality of RegPSO across Mathematical benchmarks with different iteration numbers

Benchmark	Dimension	No. particle		No. of iterations					
				50	100	150	200	250	800
Ackley	10	30	Mean	2.0427	0.69939	0.14082	0.09578	0.0703	4.6915E-
						6	4	7	
			min	1.9482	0.63282	0.11526	0.06006	0.0560	1.606E-7
						6	9		
			max	2.1371	0.76596	0.16637	0.13151	0.0845	8.7023E-
							9	7	
			std	0.13359	0.09414	0.03614	0.05051	0.0201	1.4519E-
					7	3	7	5	7
Griewangk	10	30	Mean	0.70807	0.52323	0.32358	0.27586	0.1958	0.009857
							4	3	
			min	0.62384	0.41003	0.2449	0.18308	0.1254	0.013861
							8		
			max	0.7923	0.63643	0.40226	0.36864	0.2662	0.058867
			std	0.11912	0.16009	0.11127	0.13121	0.0995	0.01552
Quadric	10	30	Mean	118.925	16.5321	3.9363	1.9285	0.8777	3.1351E-
				4			2	10	
			min	54.6702	16.1066	2.9926	0.77378	0.2330	6.0537E-
							9	11	
			max	183.180	16.9576	4.8799	3.0832	1.5223	9.5804E-
				5					10
			std	90.8706	0.60178	1.3345	1.633	0.9116	2.2243E-
							5	10	
Quartic Noisy	10	30	Mean	0.02952	0.01595	0.01309	0.00740	0.0057	5.7801E-
				2	5	3	2	8	19
			min	0.02867	0.01401	0.01217	0.00685	0.0047	
				6	2	4	2		
			max	0.03036	0.01789	0.01401	0.00795	0.0068	
				7	8	2	2	5	
			std	0.00119	0.00274	0.0013	0.00077	0.0015	
				6	8		8	2	
Rastrigin	10	30	Mean	17.0199	8.2907	7.9991	7.9822	7.5733	2.6824E-
									11
			min	13.2245	8.256	7.9812	7.9753	7.1779	0
			max	20.8152	8.3254	8.017	7.9892	7.9686	1.3337E-
									9
			std	5.3675	0.04908	0.02533	0.00982	0.5590	1.886E-
					2	7	6	5	10
Rosenbrock	10	30	Mean	206.476	108.674	88.7519	88.0642	85.750	0.003935
				8	3			7	1
			min	190.928	104.681	78.4269	77.0515	72.424	1.7028E-
				6	3			6	5
			max	222.025	112.667	99.0768	99.0768	99.076	0.018039
				1	3			8	

			std	21.9886	5.6469	14.6017	15.5742	18.845	0.004137
								9	5
Weighted	10	30	mean	0.02652	0.00472	0.00062	0.00051	0.0002	9.8177E-
Sphere				5	9	6	8	8	14
			min	0.02249	0.00105	0.0006	0.00051	0.0002	1.9112E-
				3				8	14
			max	0.03055	0.00840	0.00065	0.00052	0.0002	2.5244E-
				7	7	5	6	9	13
			std	0.00570	0.00520	4.09E-	1.13E-	1.3E-	5.4364E-
				2	2	05	05	05	14

Observing Tables 7 and 8, it is clear to notice the drop in values with an increasing number of particles and number of iterations respectively for all the benchmarks. This indicates the capability of the code to minimise the seven mathematical benchmark functions consisting of uni, bi and multi-modal functions by explicitly exploring and exploiting the search space. It is also interesting to observe the consistency of the code across all the benchmarks considered.

4.3 Case studies of Optimization Problems

To demonstrate the functionality of the Optimisation tool (MooOpT4FPSO), two case studies considering the validated model described in section 3 were used to optimise the mooring line parameters of the turret FPSO with 4x3 and 3x3 configurations with 12 and 9 mooring lines.

4.3.1 Case of Turret FPSO with Twelve Taut Mooring Lines

Figure 9 illustrates the optimization results from MooOpT4FPSO for turret FPSO with 12 lines. The GUI illustrate the optimised parameters to maintain a platform of 15m and a mooring azimuth layout.

Furthermore, Tables 9 and 10 illustrate the optimal solutions for the mooring design variables.

Table 9 shows the comparison of original and optimised mooring line azimuth angles. Other parameters presented are shown in Table 10. Which shows the reduction in line length and diameter and mooring radius, with a consequent reduction in platform offset from 40.8m to 14.99m as specified (target platform offset). This is equivalent to a 63.3% reduction in the platform offset. In addition, the reduction in line length and diameter comes with a reduction in line material and resulting payload. Also, a reduction in mooring radius will yield a consequent reduction in line tension.

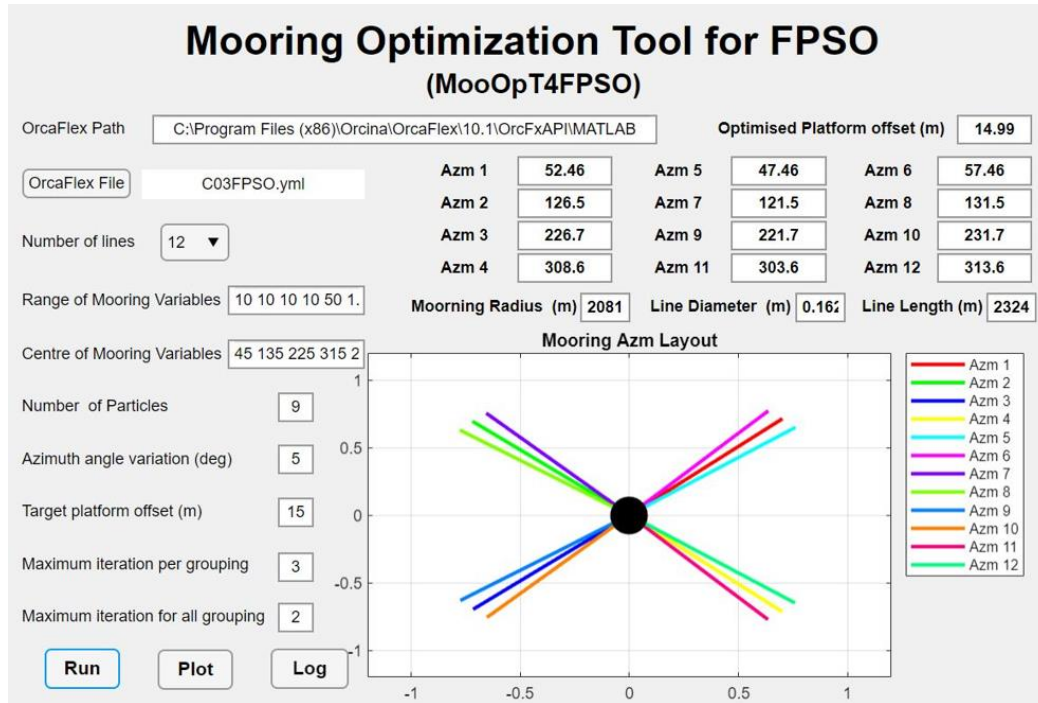


Figure 9: Complete optimization result for turret FPSO with 12 mooring line

Table 9: Comparison of original and Optimised mooring Azimuth angles

Line	Azimuth (°)	
	Original	Optimized
Line 1	45	52.46
Line 2	135	126.5
Line 3	225	226.7
Line 4	315	308.6
Line 5	40	47.46
Line 6	50	57.46
Line 7	130	121.5
Line 8	140	131.5
Line 9	220	221.7
Line 10	230	231.7
Line 11	310	303.6
Line 12	320	313.6

Table 10: Comparison of original and Optimized Mooring length, line diameter and Mooring radius

	Original	Optimized	%Difference
Mooring Length (m)	2438	2324	4.7
Diameter(mm)	170	162	4.7
Mooring Radius(m)	2090	2081	0.43
Surge Offset	40.8	14.99	63.3

4.3.2 Case of Turret FPSO with Nine Taut Mooring Lines

In the case of turret moored FPSO with 9 mooring lines, the 4th row of azimuth angles consisting of lines #4, #11 and #12 as shown in the GUI are not considered as shown in Figure 10. Tables 10 and 11 compares original and optimized line parameters from MooOpT4FPSO. In each case, the optimized parameters are better than the original in terms of reduction in line length and diameter.

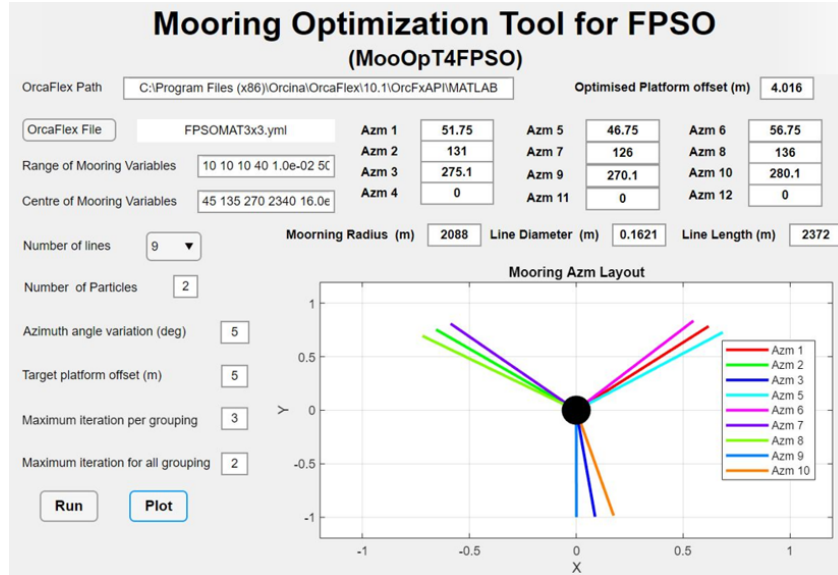


Figure 10: Complete optimization result for turret FPSO with 9 mooring lines

Table 11: Comparison of original and Optimised mooring Azimuth angles

Line	Azimuth (°)	
	Original	Optimized
Line 1	50	51.75
Line 2	135	131
Line 3	270	275.1
Line 4	45	46.75
Line 5	55	56.75
Line 6	130	126
Line 7	140	136
Line 8	265	270.1
Line 9	270	280.1

Table 12: Comparison of original and Optimized Mooring length, line diameter and Mooring radius

	Original	Optimized	%Difference
Mooring Length (m)	2438	2372	3
Diameter(mm)	170	162.1	4.6
Mooring Radius(m)	2090	2088	0.1
Surge Offset	44.2	23.21	47.5

4.3.3 Case of Turret FPSO with Twelve Catenary Mooring Lines

The optimization result for a turret FPSO with 12 catenary mooring lines is illustrated in Figure 11. The results indicated optimized mooring parameters required to maintain the platform within a 30-meter offset as defined during the analysis. Detailed comparisons are presented in Tables 13 and 14.

Table 13 compares the mooring line azimuth angle of the original and optimized models. On the other hand, Table 14 compares the mooring line length, mooring radius, and line diameter of the original and optimised model. In each case, the optimised parameters present better line parameters, with the 3.4%, 5.2% and 2.8% reduction in mooring line length, diameter, and mooring radius, respectively on every single line. In addition, a significant reduction in platform offset of 67.7% was recorded. The optimised result is consistent with the ones presented for taut moorings thereby confirming the capability of the tool.

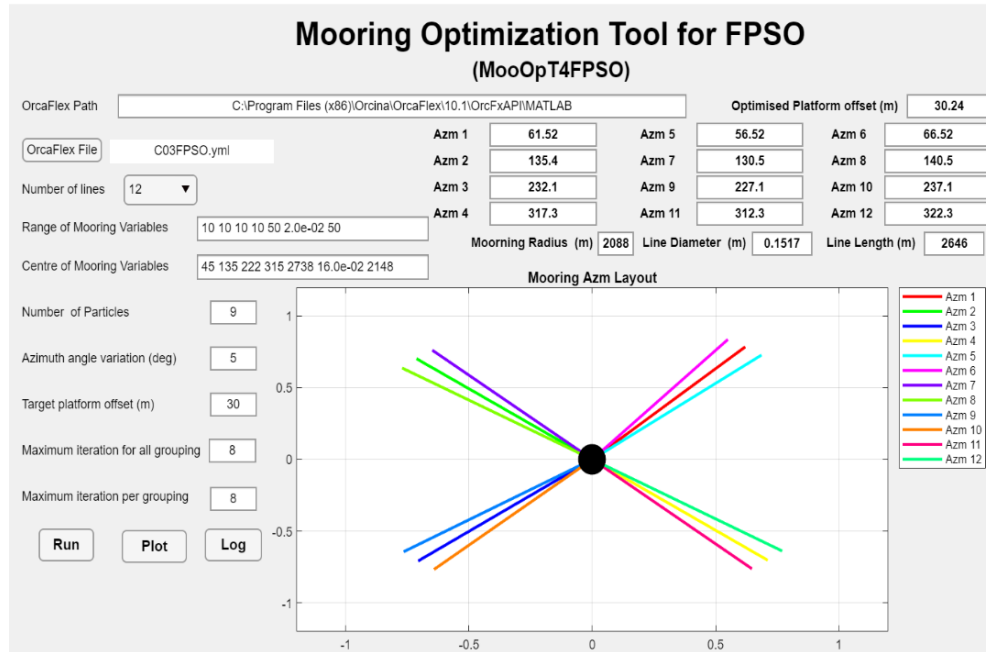


Figure 11: Complete Optimization result for turret FPSO with 12 Catenary mooring lines

Table 13: Comparison of original and Optimized mooring Azimuth angles

Line	Azimuth (°)	
	Original	Optimized
Line 1	45	61.52
Line 2	135	135.4
Line 3	225	232.1
Line 4	315	317.0
Line 5	40	56.53

Line 6	50	66.52
Line 7	130	130.4
Line 8	140	140.4
Line 9	220	227.1
Line10	230	237.1
Line11	310	312.0
Line12	320	322.0

Table 14: Comparison of original and Optimized Mooring length, line diameter and Mooring radius

	Original	Optimized	%Difference
Mooring Length (m)	2738	2646	3.4
Diameter(mm)	160	151.7	5.2
Mooring Radius(m)	2148	2088	2.8
Surge Offset	93.4	30.2	67.7

4.3.4 Case of Turret FPSO with Nine Catenary Mooring Lines

Figure 12 illustrates optimised results of turret FPSO with 9 catenary mooring lines from MooOpt4FPSO.

The detail of the results is further elaborated in Tables 15 and 16. The variations of azimuth angles as illustrated in Table 15 has a direct influence on mooring line length, diameter and the mooring radius as shown in Table 16. Most importantly the resulting optimised line parameters have successfully reduced the platform offset by 64.5%.

This is consistent with the results obtained by other mooring configurations presented using taut moorings.

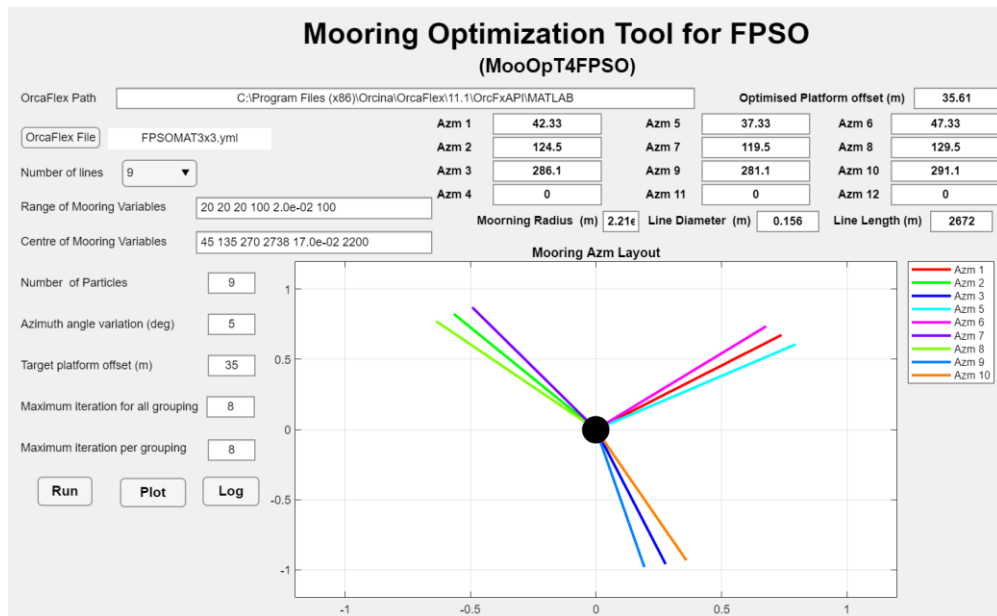


Figure 12: Complete Optimization result for turret FPSO with 9 Catenary mooring lines

Table 15: Comparison of original and Optimised mooring Azimuth angles

Line	Azimuth (°)	
	Original	Optimized
Line 1	50	42.33
Line 2	135	124.45
Line 3	270	286.10
Line 4	45	37.33
Line 5	55	47.33
Line 6	130	119.45
Line 7	140	129.45
Line 8	265	281.1
Line 9	270	291.1

Table 16: Comparison of original and Optimized Mooring length, line diameter and Mooring radius

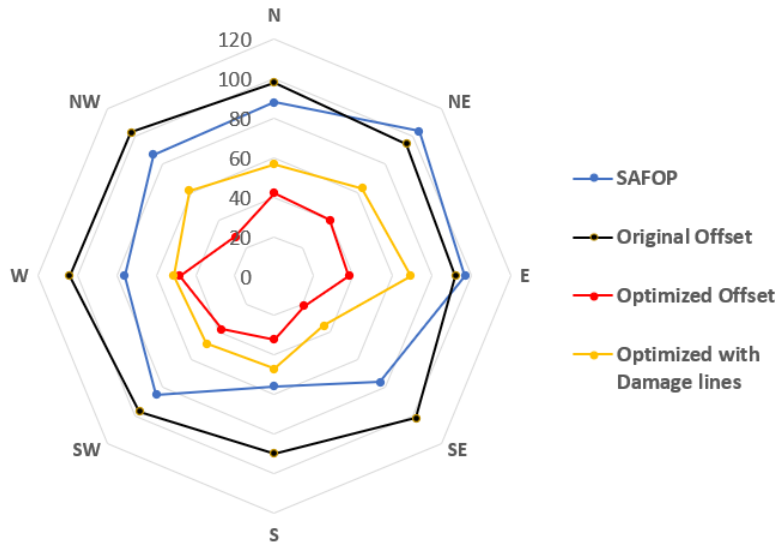
	Original	Optimized	%Difference
Mooring Length (m)	2738	2672	2.40
Diameter(mm)	160	156.1	2.40
Mooring Radius(m)	2148	2096	2.42
Surge Offset	100.2	35.6	64.5

4.4 Evaluation of Optimized Mooring Offset with riser SAFOP in intact and Damage Conditions.

4.4.1 Comparison with FPSO with **Twelve Taut** Mooring Lines

The superimposed SAFOP and offset diagram in **Figure 13** compare the maximum offset of the original model with 12 taut lines and optimized mooring configurations (intact and damaged) with the SAFOP limits to ensure the integrity of the risers in all 8 directions considered. From these figures, it can be observed that the optimized mooring configurations maintain the platform within the SAFOP zone of the risers even in the event of a line failure.

1
2
3
4 541
5
6
7
8
9
10
11
12
13
14
15
16
17
18
19
20
21
22



23 542
24
25 543
26 544
27

Figure 13: Comparison of SAFOP and Optimised offset diagrams for FPSO with 12 mooring lines with damaged lines.

28 545 4.4.2 Comparison with Turret FPSO with **Nine Taut** Mooring Lines

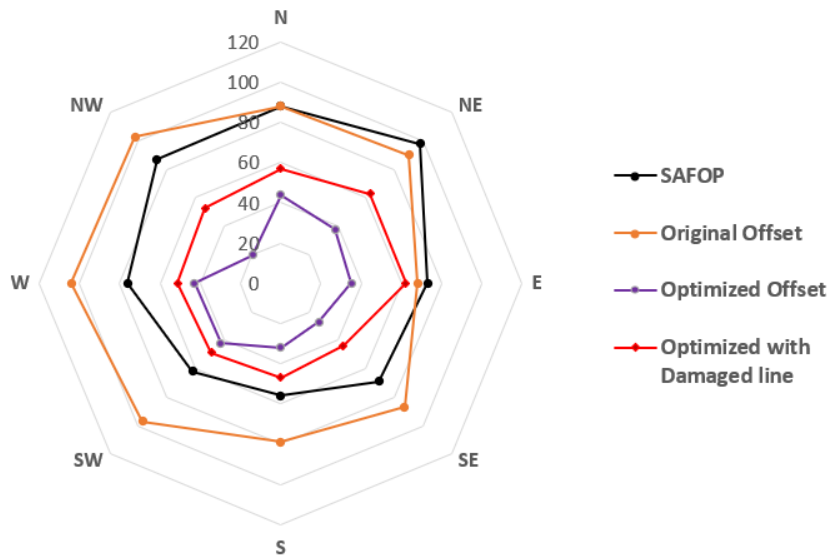
29
30 546
31
32 547

Figures 14 compares the platform offset of the original FPSO with nine taut moorings, the optimised (intact and damaged) with the SAFOP.

33
34 548
35
36 549
37 550

It can be observed for both intact and damaged conditions, the optimised platform offsets in all directions are maintained within the riser SAFOP. While for the original model, platform offset is only maintained in two directions (NE and E).

38
39
40
41
42
43
44
45
46
47
48
49
50
51
52
53
54
55



56 551
57
58 552
59 553
60
61
62
63
64
65

Figure 14: Comparison of SAFOP and Optimized offset diagrams for FPSO with 9 mooring lines with damaged lines.

1
2
3
4
5
6
7
8
9
10
11
12
13
14
15
16
17
18
19
20
21
22
23
24
25
26
27
28
29
30
31
32
33
34
35
36
37
38
39
40
41
42
43
44
45
46
47
48
49
50
51
52
53
54
55
56
57
58
59
60
61
62
63
64
65

4.4.3 Comparison with Turret FPSO with Twelve Catenary Mooring Lines

Figures 15 illustrate the comparison of platform offset for the original and optimised model from MooOpT4FPSO. This case considers catenary mooring lines in intact and damaged condition.

The optimized platform offset can be observed to be within the SAFOP in all 8 directions while the platform offset from the original model can be seen to go beyond the SAFOP in 4 directions (NW, W, SW, S).

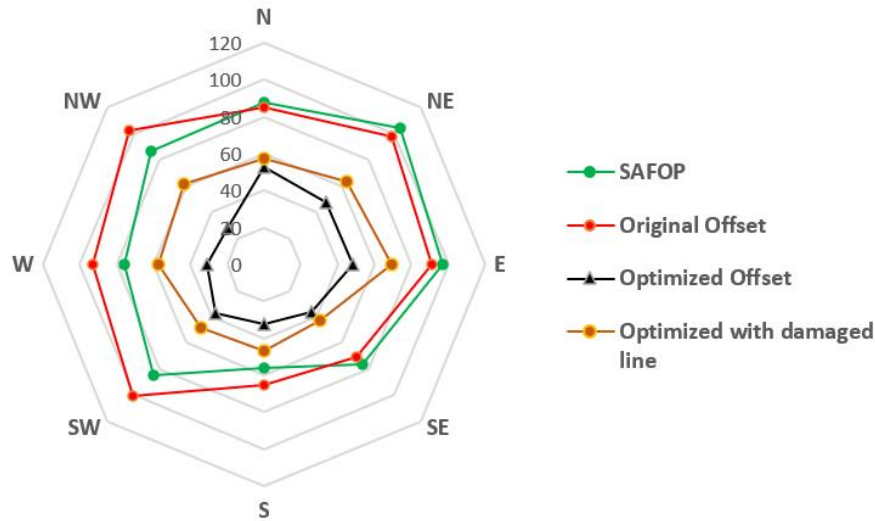


Figure 15: Comparison of SAFOP and Optimised offset diagrams for FPSO with 12 catenary mooring lines with a damaged line.

4.4.4 Comparison with Turret FPSO with Nine Catenary Mooring Lines

In this case, Figure 16 compare the platform offset of turret FPSO with 9 catenary lines.

Similar to what was observed in Figure 15, the optimised offset can be observed to be within the SAFOP in all 8 directions compared to the original. Also, in the case of damage, the optimised offset is maintained within the riser SAFOP.

This infers the efficiency of the tool in providing mooring parameters that ensure platform offset is maintained within the risers' safe operation zones.

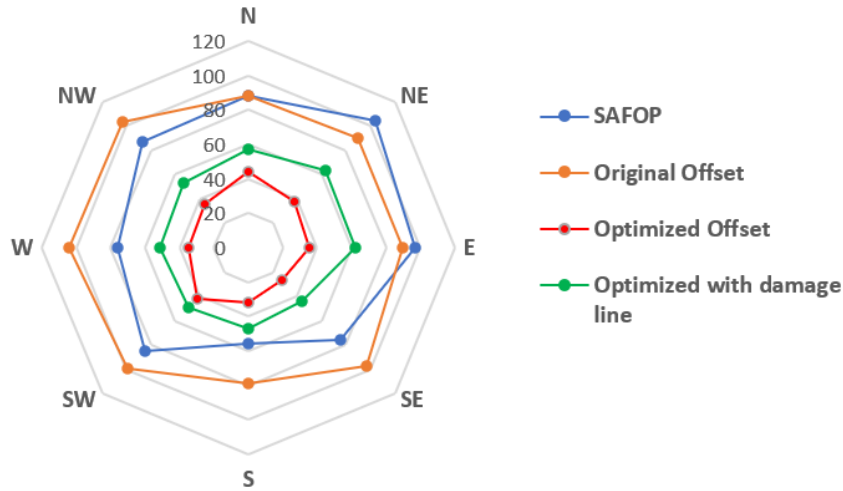


Figure 16: Comparison of SAFOP and Offset diagrams for FPSO with 9 Catenary mooring lines

5 Conclusion

In this paper, we presented an optimisation procedure of mooring line parameters for a turret moored FPSO using a Mooring Optimisation Tool for FPSO (MooOpT4FPSO). The tool is an integration of the Regrouping particle swarm optimisation (RegPSO) algorithm and a commercial software OrcaFlex. In addition, the integrated riser-mooring design methodology has been incorporated to take into consideration the interaction of the riser, mooring and the FPSO hull. The superimposed riser safe operation zone (SAFOP) and the platform offset diagram are used to assess and ensure that maximum platform offset is maintained within the riser safe operating zone. The specific conclusion from this study are as follows:

- 1) The Optimization tool has successfully simultaneously optimized mooring line length (mid-segment), line diameter, mooring radius, and azimuth angles of turret FPSO while ensuring platform excursions are maintained within the riser safe operation zone, which is very important.
- 2) The tool has the computational capability of optimizing mooring line parameters of turret FPSO with 12 and 9 mooring lines to achieve target platform offset.
- 3) From the optimised results, the application of the tool in mooring design can bring a reduction in line material and consequently the overall project cost, in addition to the reduction of payload exerted on the platform.

Acknowledgements

The authors acknowledged the Universiti Teknologi PETRONAS, Malaysia for supporting this research under YUTP 015LC0-116.

References

- [1] I. A. Ja'e, M. O. A. Ali, A. Yenduri, Z. Nizamani, and A. Nakayama, "Optimisation of mooring line parameters for offshore floating structures: A review paper," *Ocean Engineering*, vol. 247, p. 110644, 2022.
- [2] B. da Fonseca Monteiro, J. S. Baioco, C. H. Albrecht, B. S. L. P. de Lima, and B. P. Jacob, "Optimization of mooring systems in the context of an integrated design methodology," *Marine Structures*, vol. 75, p. 102874, 2021.
- [3] O. Montasir, A. Yenduri, and V. Kurian, "Mooring system optimisation and effect of different line design variables on motions of truss spar platforms in intact and damaged conditions," *China Ocean Engineering*, vol. 33, no. 4, pp. 385-397, 2019.
- [4] S. F. Senra, F. N. Correa, B. P. Jacob, M. r. M. Mourelle, and I. a. Q. Masetti, "Towards the Integration of Analysis and Design of Mooring Systems and Risers: Part I—Studies on a Semisubmersible Platform," in *International Conference on Offshore Mechanics and Arctic Engineering*, 2002, vol. 36118, pp. 41-48.
- [5] S. Mehdi and A. Rezvani, "Mooring optimization of floating platforms using a genetic algorithm," *Ocean Engineering*, vol. 34, no. 10, pp. 1413-1421, 2007, doi: 10.1016/j.oceaneng.2006.10.005.
- [6] S. A. R. D. S. Maffra, M. A. C. Pacheco, and I. F. M. g. de Menezes, 1, 3., "Genetic Algorithm Optimization for Mooring Systems," *Generations*, vol. 1, no. 3, 2003.
- [7] J. J. C. Alonso, F. M. M. Ivan, and F. M. Luiz, "Mooring Pattern Optimization using Genetic Algorithms " in *6th World Congresses of Structural and Multidisciplinary Optimization*, Rio de Janeiro, Brazil, 2005, pp. 1-9.
- [8] M. Liang, X. Wang, S. Xu, and A. Ding, "A shallow water mooring system design methodology combining NSGA-II with the vessel-mooring coupled model," *Ocean Engineering*, vol. 190, Oct 15 2019, Art no. 106417, doi: 10.1016/j.oceaneng.2019.106417.
- [9] B. da Fonseca Monteiro, C. H. Albrecht, and B. P. Jacob, "Application of the particle swarm optimization method on the optimization of mooring systems for offshore oil exploitation," in *Proceedings of Second International Conference on Engineering Optimization*, 2010.
- [10] B. Da Fonseca Monteiro, M. H. A. De Lima Jr, C. H. Albrecht, B. De Souza Leite, P. De Lima, and B. P. Jacob, "Mooring optimization of offshore floating systems using an improved particle swarm optimization method," 2013, vol. 1, doi: 10.1115/OMAE2013-11096. [Online]. Available:
- [11] B. D. F. Monteiro, J. S. Baioco, C. H. Albrecht, B. S. L. P. de Lima, and B. P. Jacob, "Optimization of mooring systems in the context of an integrated design methodology," *Marine Structures*, Article vol. 75, 2021, Art no. 102874, doi: 10.1016/j.marstruc.2020.102874.
- [12] B. F. Monteiro, A. A. de Pina, J. S. Baioco, C. H. Albrecht, B. S. L. P. de Lima, and B. P. Jacob, "Toward a methodology for the optimal design of mooring systems for floating offshore platforms using evolutionary algorithms," *Marine Systems and Ocean Technology*, Article vol. 11, no. 3-4, pp. 55-67, 2016, doi: 10.1007/s40868-016-0017-8.
- [13] *Analysis of Stationkeeping Systems for Floating Structures*, A. Design, 2005.
- [14] A. R. C. Girón, F. N. Corrêa, A. O. V. Hernández, and B. P. Jacob, "An integrated methodology for the design of mooring systems and risers," *Marine Structures*, vol. 39, pp. 395-423, 2014.
- [15] B. Seymour, H. Zhang, and C. Wibner, "Integrated Riser and Mooring design for the P-43 and P-48 FPSOs," in *Offshore Technology Conference*, 2003: Offshore Technology Conference.
- [16] *Offshore Standard: Position Mooring*, D. N. Veritas, 2010.
- [17] P. Chakrabarti, R. Chandwani, and I. Larsen, "Analyzing the effect of integrating riser/mooring line design," in *Proceedings of OMAE*, 1996: American Society of Mechanical Engineers, New York, NY (United States).

1
2
3
4
5
6
7
8
9
10
11
12
13
14
15
16
17
18
19
20
21
22
23
24
25
26
27
28
29
30
31
32
33
34
35
36
37
38
39
40
41
42
43
44
45
46
47
48
49
50
51
52
53
54
55
56
57
58
59
60
61
62
63
64
65

[18] D. Garrett, J. Chappell, R. Gordon, and Y. Cao, "Integrated Design of Risers and Moorings," in *Deepwater Mooring Systems: Concepts, Design, Analysis, and Materials*, 2003, pp. 300-315.

[19] F. c. N. Correa, S. F. Senra, B. P. Jacob, I. a. Q. Masetti, and M. r. M. Mourelle, "Towards the Integration of Analysis and Design of Mooring Systems and Risers: Part II—Studies on a DICAS System," in *International Conference on Offshore Mechanics and Arctic Engineering*, 2002, vol. 36118, pp. 291-298.

[20] *Design and Analysis of Stationkeeping Systems for Floating Structures*, API, Washington DC, 2005.

[21] George I. Evers and M. B. Ghalia, "Regrouping Particle Swarm Optimization:A New Global Optimization Algorithm with Improved Performance Consistency Across Benchmarks," in *IEEE International Conference on Systems, Man, and Cybernetics*, San Antonio, TX, USA, 2009, pp. 3901-3908.

[22] M. Kaucic, "A multi-start opposition-based particle swarm optimization algorithm with adaptive velocity for bound constrained global optimization," *Journal of Global Optimization*, vol. 55, no. 1, pp. 165-188, 2013.

[23] F. Van Den Bergh, "An analysis of particle swarm optimizers," University of Pretoria, 2007.

[24] M. Kim, B. Koo, R. Mercier, and E. Ward, "Vessel/mooring/riser coupled dynamic analysis of a turret-moored FPSO compared with OTRC experiment," *Ocean Engineering*, vol. 32, no. 14-15, pp. 1780-1802, 2005.

[25] B. Liu, L. Wang, Y.-H. Jin, F. Tang, and D.-X. Huang, "Improved particle swarm optimization combined with chaos," *Chaos, Solitons & Fractals*, vol. 25, no. 5, pp. 1261-1271, 2005.

[26] A. P. Piotrowski, J. J. Napiorkowski, and A. E. Piotrowska, "Population size in particle swarm optimization," *Swarm and Evolutionary Computation*, vol. 58, p. 100718, 2020.